

10. RELATIONSHIP BETWEEN SEDIMENT GRANULOMETRY AND THE PRESENCE OF GAS HYDRATE ON HYDRATE RIDGE¹

X. Su,² C.-B. Song,³ and N.-Q. Fang²

ABSTRACT

Sediments from above the bottom-simulating reflector in eight holes drilled during Ocean Drilling Program Leg 204 were analyzed to understand how sediment grain-size compositions correlate with the presence of gas hydrates on Hydrate Ridge. The results showed that all samples studied fall into the 1- to 148- μm size range. Silt is the dominant component (60%–75%), with <35% clay and <5% sand. The presence of gas hydrate generally correlates to sediment layers with >0.5%–5% sand; however, the presence of gas hydrate is also related to layers containing <0.5% sand but with increasing silt.

Abundant statistical data were obtained from correlations between 71 grain size intervals and the infrared thermal anomalies in Leg 204 holes. Values of Pearson's correlation coefficients are low (<0.478), probably indicating that variation in grain size is of certain importance for controlling the presence of gas hydrates. The statistical results showed the trend that the coarser the grain size, the more abundant the presence of gas hydrate, and vice versa, within correlated grain-size intervals at most Leg 204 sites. The exception to this is at Sites 1249 and 1250, where the presence of gas hydrate is significantly controlled by rapid supply of gas and fluid flow. Statistically, at most Leg 204 sites the presence of gas hydrate is related to a grain-size interval of 10–148 μm . Three groups of Leg 204 sites were recognized. At the sites on the southern summit area, presence of gas hydrate correlates with coarse silt to fine sand, whereas at the two sites in the slope basin area, gas hydrate is related to the very fine silt fraction. This implies that there are more

¹Su, X., Song, C.-B., and Fang, N.-Q., 2006. Relationship between sediment granulometry and the presence of gas hydrate on Hydrate Ridge. *In* Tréhu, A.M., Bohrmann, G., Torres, M.E., and Colwell, F.S. (Eds.), *Proc. ODP, Sci. Results*, 204, 1–30 [Online]. Available from World Wide Web: <http://www-odp.tamu.edu/publications/204_SR/VOLUME/CHAPTERS/115.PDF>. [Cited YYYY-MM-DD]

²Department of Geology, School of Marine Geosciences, China University of Geosciences, Xueyuan Road 29, Beijing 100083, People's Republic of China. Correspondence author: xsu@cugb.edu.cn

³Guangzhou Marine Geological Survey, Guangzhou 510075, People's Republic of China.

Initial receipt: 7 February 2005

Acceptance: 12 March 2006

Web publication: 21 August 2006

Ms 204SR-115

lithologic control factors (e.g., structural and sedimentary histories) controlling the presence of gas hydrate in the study area.

INTRODUCTION

Gas hydrate is an icelike compound that contains methane and other low-molecular weight gases in a lattice of water molecules. Submarine gas hydrate is commonly preserved in sediments near the seafloor at water depths >300 m (Kvenvolden and Lorensen, 2001). Earlier studies assumed that submarine gas hydrate generally occurs in relatively coarse grained sediments (Ginsburg and Soloviev, 1997; Kraemer et al., 2000). Ginsburg et al. (2000) conducted granulometric analyses on sediments from Ocean Drilling Program (ODP) Leg 164 sites on the Blake Outer Ridge and found that the zone of negative anomalies of pore water chlorinity (a proxy for gas hydrate presence) was confined to the interval of relatively coarser grained sediments. During ODP Leg 204, sediments were drilled on Hydrate Ridge, and Shipboard Scientific Party (2003) found that lithology is a major factor influencing gas hydrate concentration and that gas hydrate is concentrated in the coarse-grained sediment layers.

Grain-size analyses of sediments from Leg 204 were carried out with the purpose to obtain more detailed granulometric characterization of those coarse-grained layers and their correlation with the presence of gas hydrate in the study area.

MATERIAL AND METHODS

Study Area and Material

Hydrate Ridge is a 25-km-long and 15-km-wide ridge in the Cascadia accretionary complex (Fig. F1A). It is characterized by a northern summit at ~600 meters below sea level (mbsl) and a southern summit at ~800 mbsl (Fig. F1B). Tréhu and Flueh (2001) suggested that gas hydrate is present throughout Hydrate Ridge based on the overall appearance of a bottom-simulating reflector (BSR); a seismic marker for the bottom boundary of gas hydrate-bearing sediments.

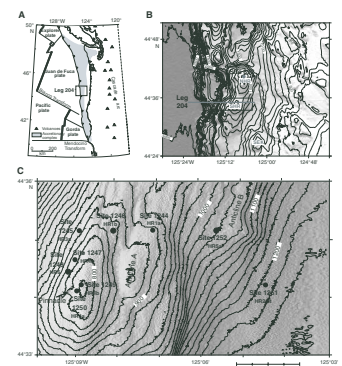
During Leg 204, nine sites were drilled in the southern summit area in the summer of 2001. These sites fall into two primary groupings (Fig. F1C). Sites 1245 and 1247–1250 form a north–south transect that documents the evolution of the southern Hydrate Ridge gas hydrate system from the north flank to the summit and explores the role of Horizon A. Sites 1244–1246, 1252, and 1251 form an east–west transect (Fig. F2) that compares the west and east flanks of southern Hydrate Ridge to the adjacent slope basin (Shipboard Scientific Party, 2003).

A total of 319 sediment samples from Leg 204 sites (Sites 1244–1246 and 1248–1252) were analyzed (Table T1). These samples are from sediment sequences above the BSR at intervals of 2–8 m (Table T1).

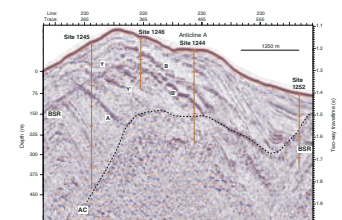
Grain-Size Analysis

Bulk sediments were diluted with a sodium hexametaphosphate (soap) solution and further dispersed for 2 min in an ultrasonic bath. After sediment samples were pretreated, grain-size distribution measurements were analyzed with a Malvern laser diffraction Mastersizer

F1. Site locations, p. 9.



F2. Seismic profile, p. 10.



T1. Site data, p. 21.

2000. Grain-surface measurements were processed by the Malvern software, and grain volumes were calculated based on a globular grain shape. The analyzer can determine a full range of particle sizes from 0.05 to 900 μm with 0.015- μm resolution and deliver various grain-size data reports (i.e., 71 grain-size intervals from 8–10 to 146–148 μm in 2- μm increments) for each sample. The reports were divided for a statistical analysis. Determination of grain-size classes followed Friedman and Sanders (1978) (Table T2).

Proxy for Gas Hydrate Presence—Infrared Anomalies

During Leg 204, various measurements were applied to trace the presence and quantity of gas hydrate in the sediments of Hydrate Ridge, including downhole logging of electrical resistivity anomalies and the identification of low-temperature anomalies by infrared (IR) camera scans immediately after core retrieval on deck. In addition, chloride concentrations were measured on pore water samples, methane/ethane ratios for vacutainer samples were determined, and gas volumes from pressure core samples were measured (Shipboard Scientific Party, 2003).

IR thermal imaging of the surface of the core liner was fully implemented during Leg 204, and it was found that discrete, strong cold anomalies in Leg 204 cores were associated with gas hydrate (Shipboard Scientific Party, 2003). Even disseminated gas hydrate (gas hydrate grains less than ~ 3 mm) distributed throughout the sediment interval is detectable on the IR images as thermal anomalies with a ΔT of $\sim 1^\circ\text{C}$ or less (Shipboard Scientific Party, 2003). Gas hydrate detected on downhole plots of the negative IR thermal anomalies in Leg 204 cores correlate well with other multiple proxies for gas hydrate presence (Shipboard Scientific Party, 2003).

This study uses these IR anomalies as the proxy for the presence of gas hydrate (Table T3).

Correlation Analysis Methods

Two methods were employed to evaluate the relationship between variations in sediment grain-size composition and the presence of gas hydrate at Leg 204 sites: a visual correlation of the data plots in Figures F3, F4, F5, F6, F7, F8, F9, and F10 and a statistical method.

For statistical analysis, we employed Pearson’s correlation coefficient; one approach of bivariate correlations in a statistics program for social sciences (SPSS) (Nie et al., 1975; Su et al., 2000). The Pearson’s correlation coefficient (r) is a usual measure of linear association which varies from -1 to $+1$, with 0 indicating no relationship. A value of $+1$ indicates perfect relationship, which is generally interpreted as “the more the x , the more the y , and vice versa.” A value of -1 is a perfect negative relationship, with a common interpretation as “the more the x , the less the y , and vice versa.” A significant correlation at the 0.05 level or at the 0.01 level is identified by this program.

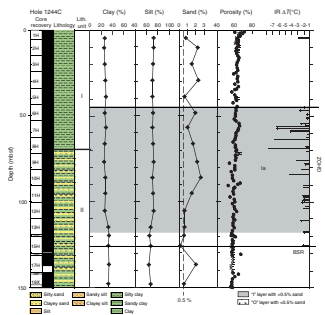
In our study, one set of variables at a Leg 204 site is the IR anomalies and the other set is the 71 grain-size intervals at the same site (Table T4). We used the significant correlations at the 0.05 level (Table T4).

It should be pointed out that the depths of the sediment samples do not exactly match those of the IR anomalies at the same site because of different sampling intervals. To match the depths, “median values” from the grain sizes of the sediment samples nearby, within our sampling intervals of 2–8 m, were created by using a method of the SPSS.

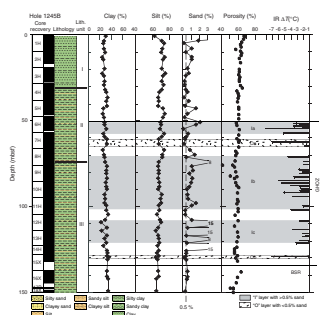
T2. Grain-size ranges, p. 22.

T3. IR anomalies, p. 23.

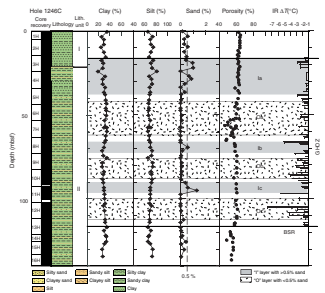
F3. Sediment grain size, Hole 1244C, p. 11.



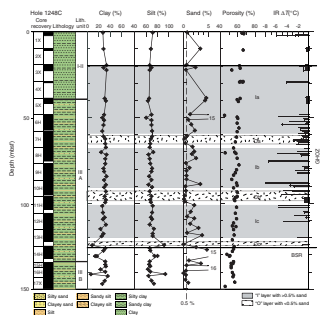
F4. Sediment grain size, Hole 1245B, p. 12.



F5. Sediment grain size, Hole 1246B, p. 13.



F6. Sediment grain size, Hole 1248B, p. 14.



This process should be considered when interpreting the statistical results.

RESULTS AND IMPLICATIONS

Table T2 shows that grain sizes of all samples studied range from 1 to 148 μm ; from clay to silt to fine sand (Friedman and Sanders, 1978). Most of these samples are dominantly composed of silt (60%–75%), with clay (5%–35%) as the second main component. The percentage of fine sand is commonly <5%; however, the composition varies greatly within the hole sequence and between the different holes.

Downhole Correlation between Sediment Granulometry and IR Anomalies

Figures F3, F4, F6, F7, F8, F9, and F10 show variations in percentage of clay, silt, and sand vs. the IR anomalies for Holes 1244C, 1245B, 1246B, 1248B, 1249C, 1250C, 1251B, and 1252A against depths, with indications of the lithostratigraphic units and the level of the BSR as described in Shipboard Scientific Party (2003). Porosity data from these cores were also plotted to examine the correlation between downhole variations in grain size and porosity.

First, we examined the correlation between variations in percentage of sand and the IR record from above the BSR and within the gas hydrate occurrence zone (GHOZ).

A number of layers are characterized by sand peaks or increasing sand. These layers were further divided into two categories: layers containing >0.5% sand were labeled “I,” and layers with <0.5% sand were labeled “O.”

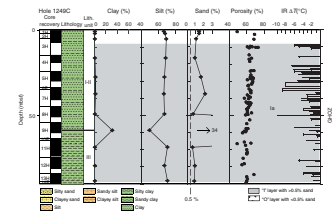
The most I layers within the GHOZ can be visually correlated with the IR anomalies: Layers Ia–Ic in Hole 1245B (Fig. F4) and those I layers in other holes (Figs. F5, F6, F7, F8, F9, F10). Figures F3, F4, F5, F6, F7, F8, F9, and F10 also show slight increasing porosity in correlation with I layers. A certain number of O layers were also correlated with IR anomalies within the GHOZ: Layers Oa–Ob in Holes 1245B, 1248C, 1250C, and 1252C (Figs. F4, F6, F8, F10). Two or three O layers are commonly present in each hole except for Hole 1249C (Fig. F7). Sediments within the GHOZ in Hole 1249C are richer in sand (>0.5%) than other Leg 204 holes and therefore do not have O layers. In addition, the silt fraction increases in the O layers (i.e., Oa–Ob layers in Holes 1250C and 1252C) (Figs. F8, F10). This possibly indicates that the silt fraction also belongs to the “coarse-grained” component that controls the presence of gas hydrate on Hydrate Ridge.

Statistical Correlation between Sediment Grain-Size Properties and IR Anomalies

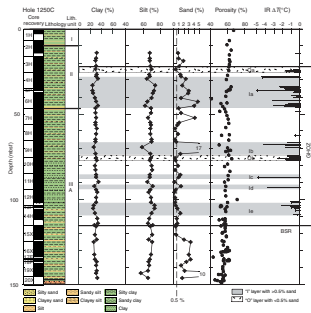
Table T4 gives the results of Pearson’s r of 71 grain-size intervals in Holes 1244C, 1245B, 1246B, 1248B, 1249C, 1250C, 1251B and 1252A. These data were further plotted in Figure F11.

The significant correlations between these variables were identified and marked with an asterisk for a 0.05 significant level by the SPSS (Table T4). Table T5 summaries the grain-size intervals that were marked with significant correlations in Leg 204 holes. In this study we focused

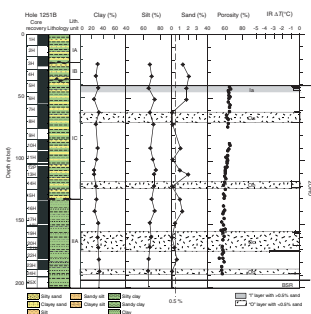
F7. Sediment grain size, Hole 1249C, p. 15.



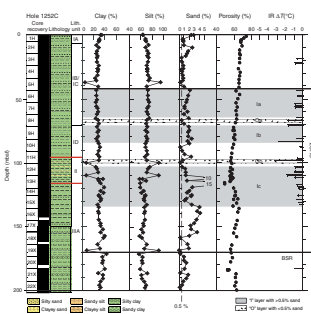
F8. Sediment grain size, Hole 1250C, p. 16.



F9. Sediment grain size, Hole 1251B, p. 17.



F10. Sediment grain size, Hole 1252C, p. 18.



T4. Correlation results, p. 25.

on the statistical features of these related variables and the grain-size intervals with significant correlations.

Generally, the values of Pearson's r for all Leg 204 holes are low, ranging from 0.478 to 0.168 or from -0.209 to -0.149 . Several reasons might explain the low values. First, the presence of gas hydrate in sediments is controlled by several factors with different natures or properties (i.e., supply of gas and fluid flow, temperatures and pressures, nature of sediments, and so on). Grain size is one of these properties. Another property is likely caused by the lack of exact depth correlations between the IR measurements and the sediment samples (see "Materials and Methods," p. 2). The mean values of the grain sizes calculated from samples in nearby holes are not accurately representative of the true grain sizes of sediments that host gas hydrates.

Both positive and negative correlations are present (Table T4; Fig. F11). Before interpretation, we should point out that the IR anomalies were given as "negative" data (Shipboard Scientific Party, 2003) (Table T4). When we read the Pearson's values in Table T4 and Figure F11, we should translate the negative correlations into the positive ones, and vice versa.

Figure F11 shows the positive linear correlation between grain sizes and values of Pearson's r within the correlated intervals in Holes 1244C, 1246B, 1248B, and 1252A, suggesting "the coarser the grain size, the more abundant IR anomalies or gas hydrate, and vice versa."

Negative correlations were found in Holes 1245B, 1249C, and 1251B. For Holes 1245C and 1251C (Fig. F11), the correlations indicate "the finer the grain sizes, the less correlation with IR anomalies or the presences of gas hydrate, and vice versa." These correlations suggest, in an opposite way, the same meaning of the positive correlations. For Hole 1249, the correlations suggest "the coarser the grain sizes, the less correlation with the presence of gas hydrate, and vice versa." According to the results of Leg 204, massive gas hydrate at Site 1249 is significantly controlled by the rapid supply of gas and fluid flow, and the stratigraphic control may be of less importance at this site than at other sites (Shipboard Scientific Party, 2003). In addition, from Figure F7 we also see the negative correlation; more IR anomalies above ~ 40 meters below seafloor (mbsf) in the sediment interval with few sand layers and fewer IR anomalies below ~ 40 mbsf where frequent turbidite layers were observed (Shipboard Scientific Party, 2003).

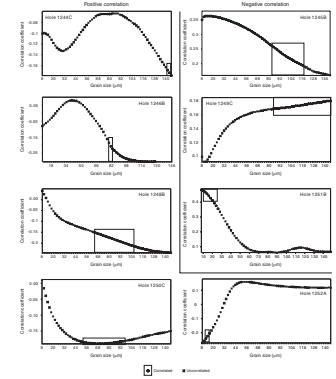
Hole 1250C is an exception among the Leg 204 holes with positive correlations, showing an nonlinear correlation between values of Pearson's r and sediment grain sizes (Fig. F11). We inferred that the presence of gas hydrate is likely controlled by other factors, such as fluid flow and gas hydrate dynamics, with similar explanations for Hole 1249C.

Table T5 shows the ranges of grain-size intervals that were marked with significant correlations in Leg 204 holes vary from 10 to 148 μm .

Three groups of holes with similar grain-size ranges were recognized and are shown in Figure F12. Group I includes Holes 1245C, 1248B, 1250C, 1249C, and 1246B, geographically located on the southern summit or close to the summit. Ranges of sediment grain size related to gas hydrate presence in these holes are large, but the major part of the range falls within 50–148 μm (Fig. F12A), which represents coarse silt to fine sand.

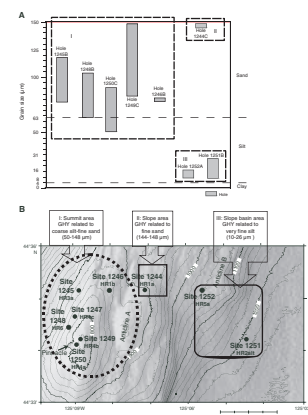
Group II includes only Hole 1244C, geographically located on the slope area (Fig. F12B). Gas hydrate in this hole is related with a very narrow range and the coarsest grain-size range among all holes studied (fine sand with sizes of 144–148 μm).

F11. Grain size and gas hydrate occurrence, p. 19.



T5. Grain size and gas hydrate, p. 30.

F12. Grain-size ranges, p. 20.



Group III includes Holes 1252A and 1251B, geographically located on the slope basin area (Fig. F12B). The presence of gas hydrate in this hole is also related to a very narrow range of grain size (very fine silt with sizes of 10–26 μm), representing the finest grain-size range related to gas hydrate.

CONCLUSIONS

In summary, grain-size data from eight Leg 204 holes drilled on Hydrate Ridge showed that all samples studied fall into the size range from 1 to ~148 μm (clay to fine sand). Silt is the dominant component of sediments above the BSR, comprising ~60%–75% of sedimentary grains. The second most abundant component is clay (<35%), whereas the sand fraction is generally <5%.

Downhole comparisons of the variations in grain size and IR anomalies suggest that gas hydrate is predominantly hosted in the sediment layers with >0.5%–5% sand (I layers); however, gas hydrate is also commonly present in the layers containing <0.5% sand but with increasing silt (O layers). This confirms that gas hydrate, in most cases, is present in coarse-grained sediments on Hydrate Ridge. Silt fraction was also considered as a component of the “coarse-grained” proportions that control gas hydrate presence on Hydrate Ridge.

Three features were observed from results derived from the statistical analysis: (1) low values of Pearson’s correlation coefficients (>0.478), (2) the presence of both positive and negative correlations, and (3) linear correlations within correlated grain-size intervals in most Leg 204 holes. The low values of Pearson’s r likely indicate that variations in grain size of sediments is of certain importance for controlling the presence of gas hydrate. In addition, the lack of exact depth correlations between the IR measurements and the sediment samples is a possible reason for the weak correlations. Generally, both the positive and negative values suggest the trend that “the coarser the grain size, the more abundant IR anomalies or gas hydrates, and vice versa” within correlated grain-size intervals at most Leg 204 sites except for at Sites 1249 and 1250. This is in agreement with the studies of Leg 204, which suggested that the presence of gas hydrate is significantly controlled by the rapid supply of gas and fluid flow, and the stratigraphic control may be of less importance at these sites than at other sites (Shipboard Scientific Party, 2003).

Statistically at most Leg 204 sites, the presence of gas hydrate at Hydrate Ridge is related to a grain-size interval of 10–148 μm . However, there is variation among the Leg 204 sites, and three groups of sites with similar ranges of grain sizes and geographic locations were recognized. At Leg 204 sites on the southern summit area, gas hydrate presence correlates with coarse silt–fine sand. At the Leg 204 sites on the slope basin area, gas hydrate is related to the very fine silt fraction. This implies that there are more lithologic control factors (e.g., structural and sedimentary histories) controlling the presence of gas hydrate in the study area.

ACKNOWLEDGMENTS

This research used samples and data provided by the Ocean Drilling Program (ODP). ODP is sponsored by the U.S. National Science Founda-

tion (NSF) and participating countries under the management of Joint Oceanographic Institutions (JOI), Inc. In particular, we thank Dr. Federica Tamburini and Dr. Bernhard Diekman for excellent advice and suggestions for improving this manuscript. Funding for this research was provided by the National Program on Key Basic Research Projects (Grant G2000046705) and the Chinese ODP committee.

REFERENCES

- Friedman, G.M., and Sanders, J.E., 1978. *Principles of Sedimentology*: New York (Wiley).
- Ginsburg, G., Soloviev, V., Matveeva, T., and Andreeva, I., 2000. Sediment grain-size control on gas hydrate presence, Sites 994, 995, and 997. In Paull, C.K., Matsumoto, R., Wallace, P.J., and Dillon, W.P. (Eds.), *Proc. ODP, Sci. Results*, 164, 237–245 [CD-ROM]. Available from: Ocean Drilling Program, Texas A&M University, College Station, TX 77845-9547, U.S.A.
- Ginsburg, G.D., and Soloviev, V.A., 1997. Methane migration within the submarine gas-hydrate stability zone under deep-water conditions. *Mar. Geol.*, 137:49–57. [doi:10.1016/S0025-3227\(96\)00078-3](https://doi.org/10.1016/S0025-3227(96)00078-3)
- Kraemer, L.M., Owen, R.M., and Dickens, G.R., 2000. Lithology of the upper gas hydrate zone, Blake Outer Ridge: a link between diatoms, porosity, and gas hydrate. In Paull, C.K., Matsumoto, R., Wallace, P.J., and Dillon, W.P. (Eds.), *Proc. ODP, Sci. Results*, 164: College Station, TX (Ocean Drilling Program), 164:229–236. [[HTML](#)]
- Kvenvolden, K.A. and Lorenson, T.D., 2001. The global occurrence of natural gas hydrate. In Paull, C.K., and Dillon, W.P. (Eds.), *Natural Gas Hydrates: Occurrence, Distribution, and Dynamics*. Geophys. Monogr., 124:3–18.
- Nie, H.H., Hull, C.H., Jenkins, J.G., Steinbrenner, K., and Bent, D.H., 1975. *SPSS: Statistical Package for the Social Sciences*: New York (McGraw-Hill).
- Shipboard Scientific Party, 2003. Leg 204 summary. In Tréhu, A.M., Bohrmann, G., Rack, F.R., Torres, M.E., et al., *Proc. ODP, Init. Repts.*, 204: College Station TX (Ocean Drilling Program), 1–75. [[HTML](#)]
- Su, M.-J., Fu, R.-H., Zhou, J.-B. et al., 2000. *Introduction to Statistic Program SPSS for Windows*: Beijing (Beijing Press of Electronic Industry), 54–81, 451–455. (in Chinese)
- Tréhu, A.M., and Flueh, E.R., 2001. Estimating the thickness of the free gas zone beneath Hydrate Ridge, Oregon continental margin, from seismic velocities and attenuation. *J. Geophys. Res.*, 106:2035–2045. [doi:10.1029/2000JB900390](https://doi.org/10.1029/2000JB900390)

Figure F1. Leg 204 study area and sites. A. Tectonic setting of Hydrate Ridge in the accretionary complex of Cascadia subduction. B. Bathymetric map of Hydrate Ridge. NHR = northern Hydrate Ridge, SHR = southern Hydrate Ridge, SEK = Southeast Knoll. C. Detailed bathymetric map of the region south of Hydrate Ridge and location of Leg 204 sites (Shipboard Scientific Party, 2003).

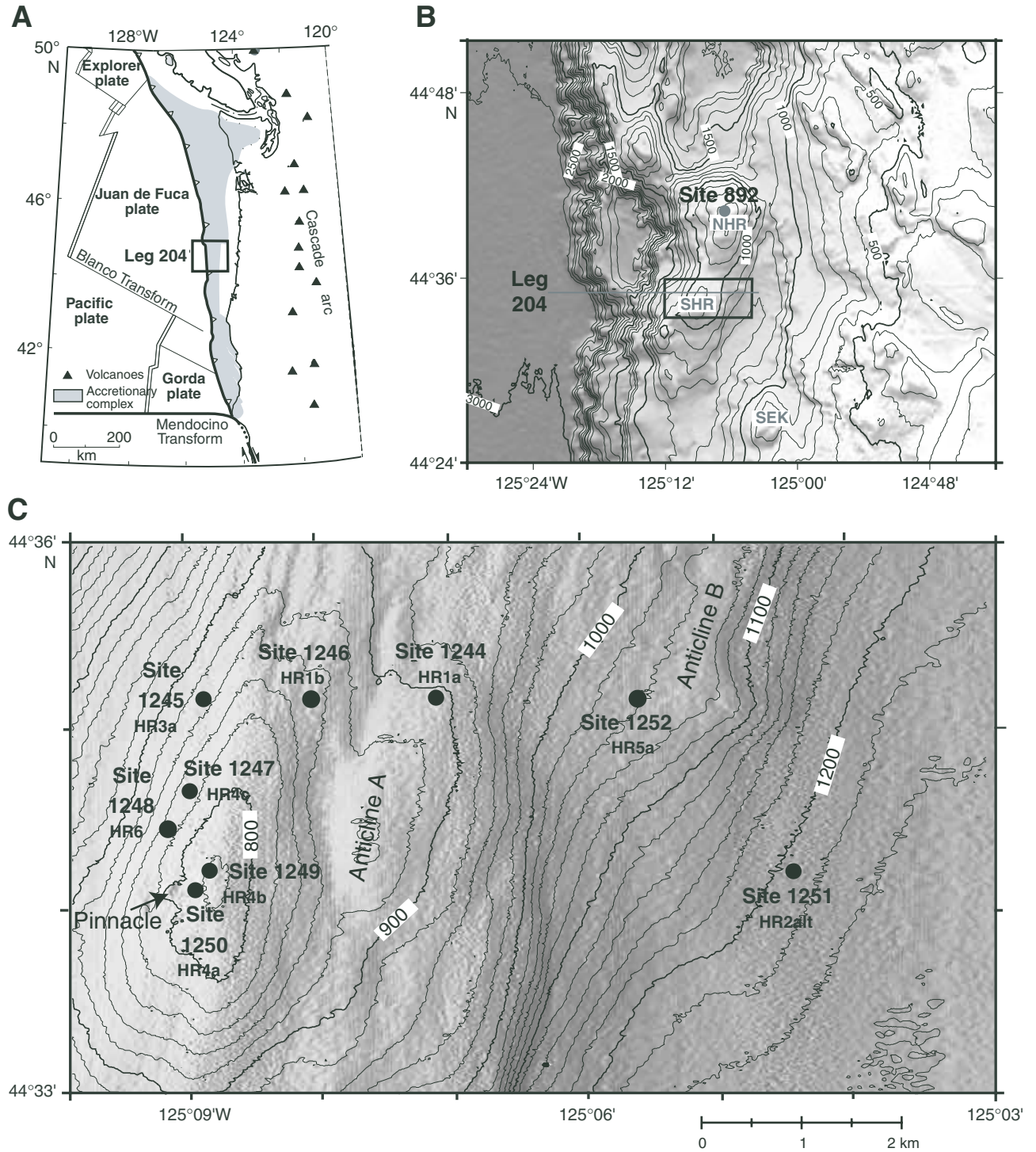


Figure F2. East-west vertical slice through the three-dimensional seismic profile showing the stratigraphic and structural setting of Sites 1244, 1246, and 1252 (Shipboard Scientific Party, 2003). AC, A, B, B', Y, Y' = seismic reflectors, BSR = bottom-simulating reflector.

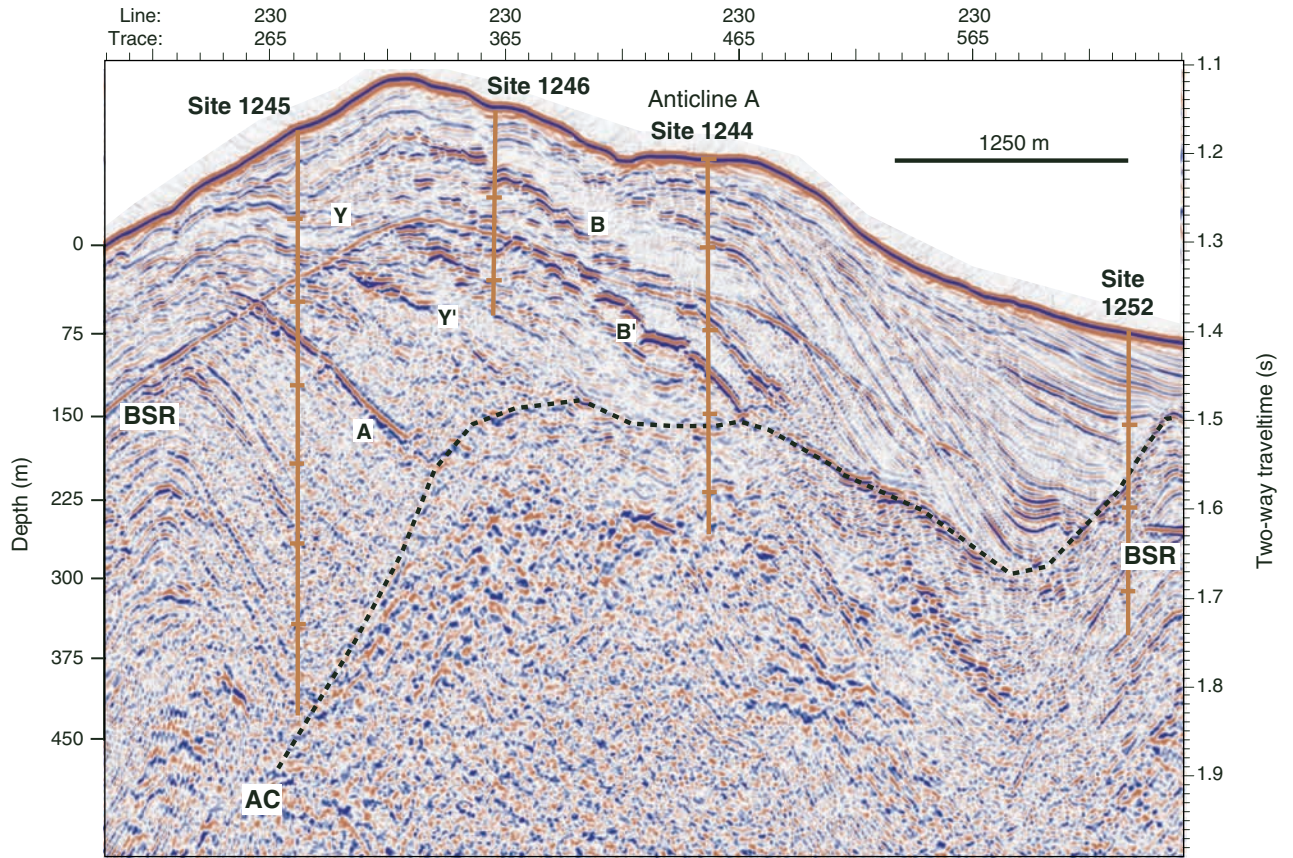


Figure F3. Downhole variation of sediment grain size within the gas hydrate occurrence zone (GHOZ) in Hole 1244C correlated with infrared thermal anomalies (IR) and porosity. BSR = bottom-simulating reflector. IR and porosity data, core recovery, lithologic units, and legends for lithology are from Shipboard Scientific Party (2003).

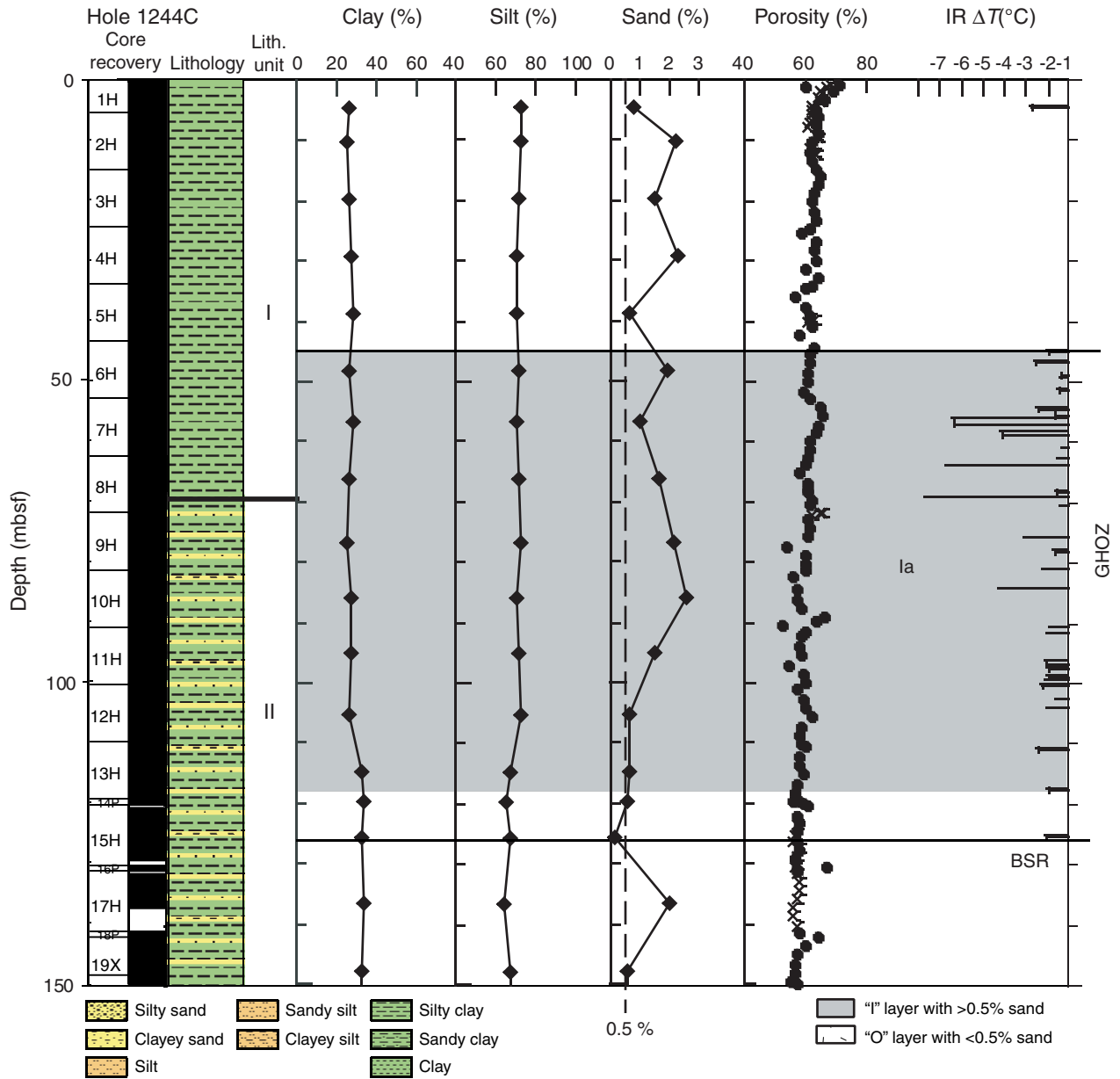


Figure F4. Downhole variation of sediment grain size within the gas hydrate occurrence zone (GHOZ) in Hole 1245B correlated with infrared thermal anomalies (IR) and porosity. BSR = bottom-simulating reflector. IR and porosity data, core recovery, lithologic units, and legends for lithology are from Shipboard Scientific Party (2003).

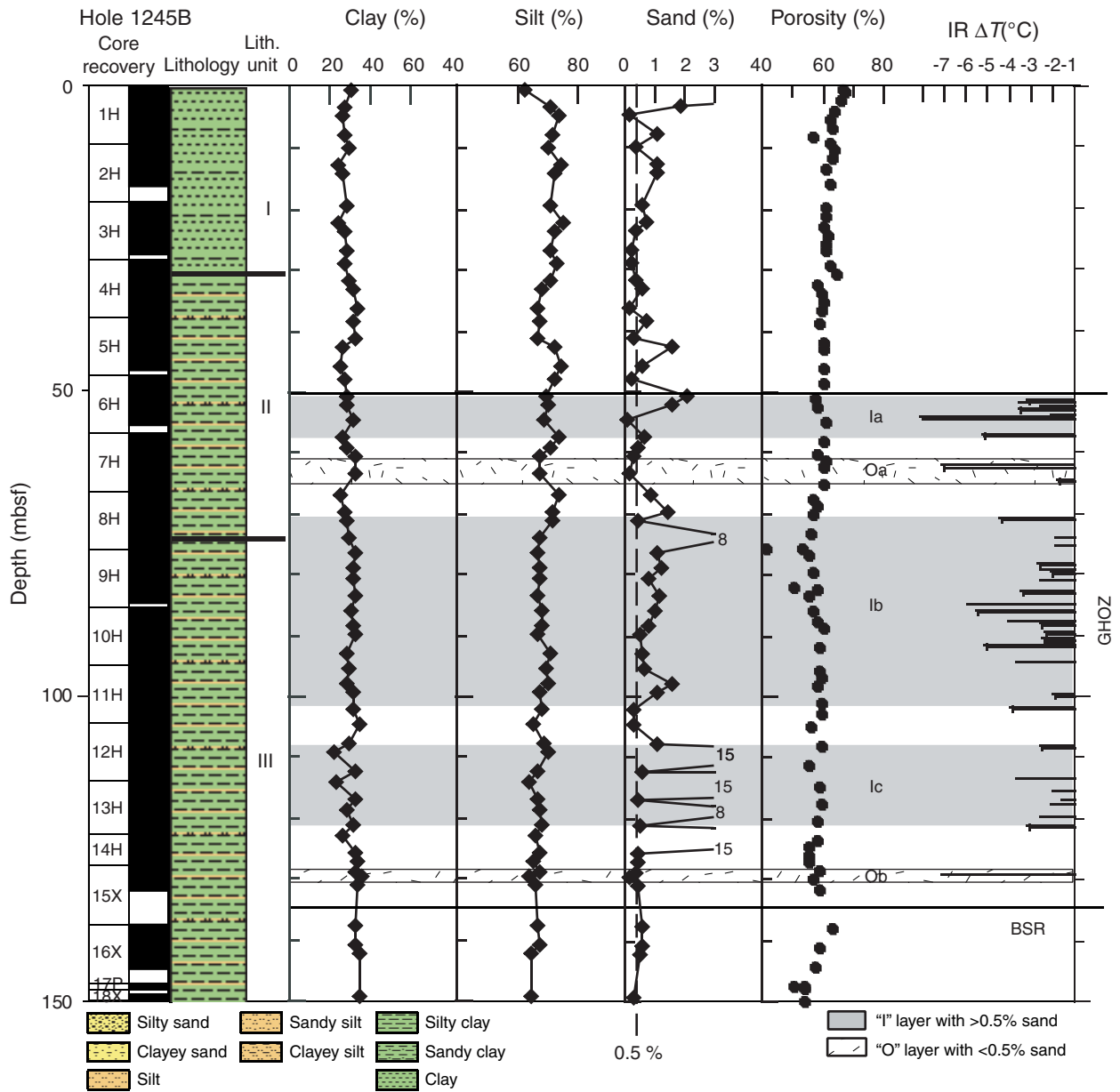


Figure F5. Downhole variation of sediment grain size within the gas hydrate occurrence zone (GHOZ) in Hole 1246B correlated with infrared thermal anomalies (IR) and porosity. BSR = bottom-simulating reflector. IR and porosity data, core recovery, lithologic units, and legends for lithology are from Shipboard Scientific Party (2003).

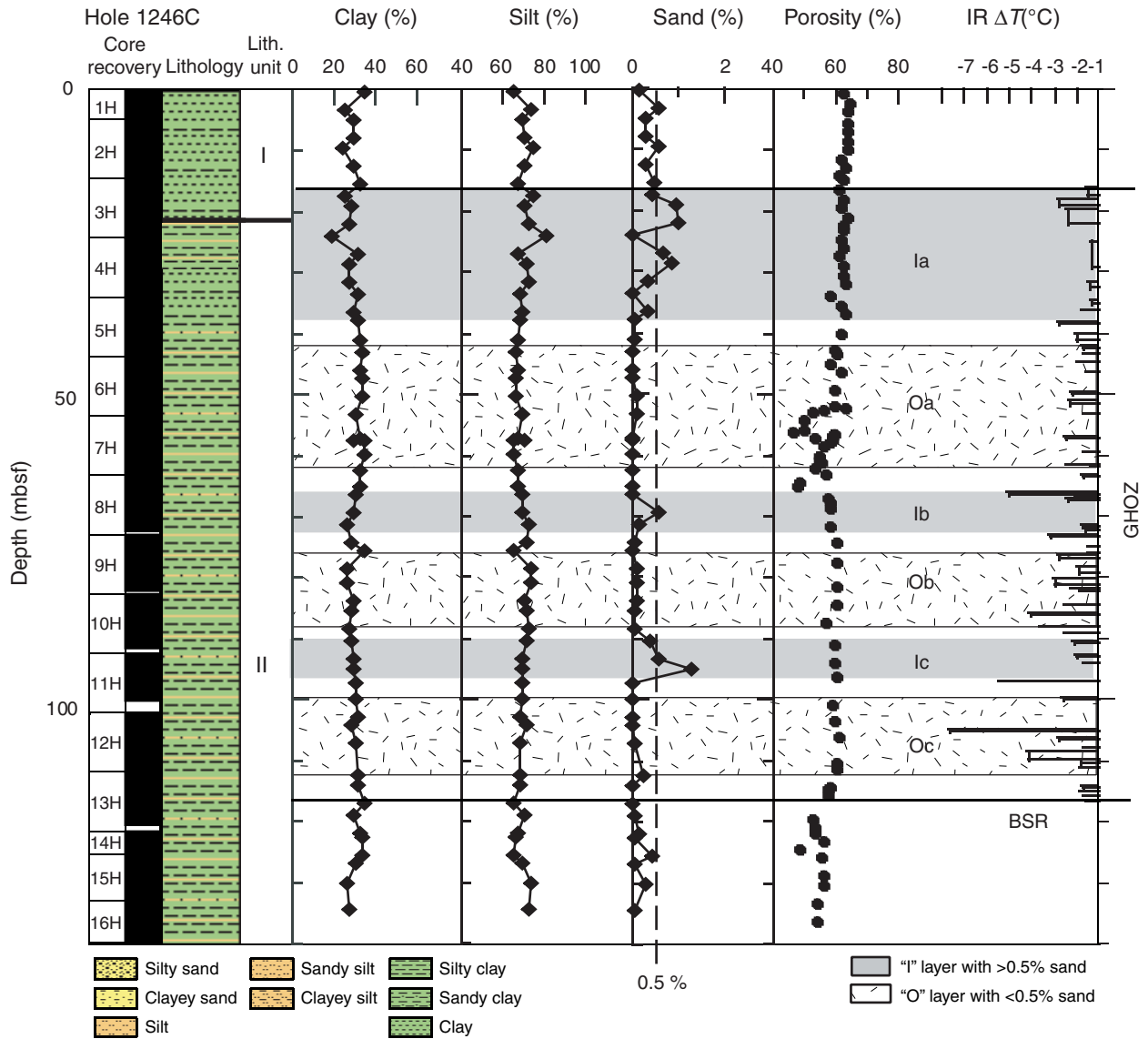


Figure F6. Downhole variation of sediment grain size within the gas hydrate occurrence zone (GHOZ) in Hole 1248B correlated with infrared thermal anomalies (IR) and porosity. BSR = bottom-simulating reflector. IR and porosity data, core recovery, lithologic units, and legends for lithology are from Shipboard Scientific Party (2003).

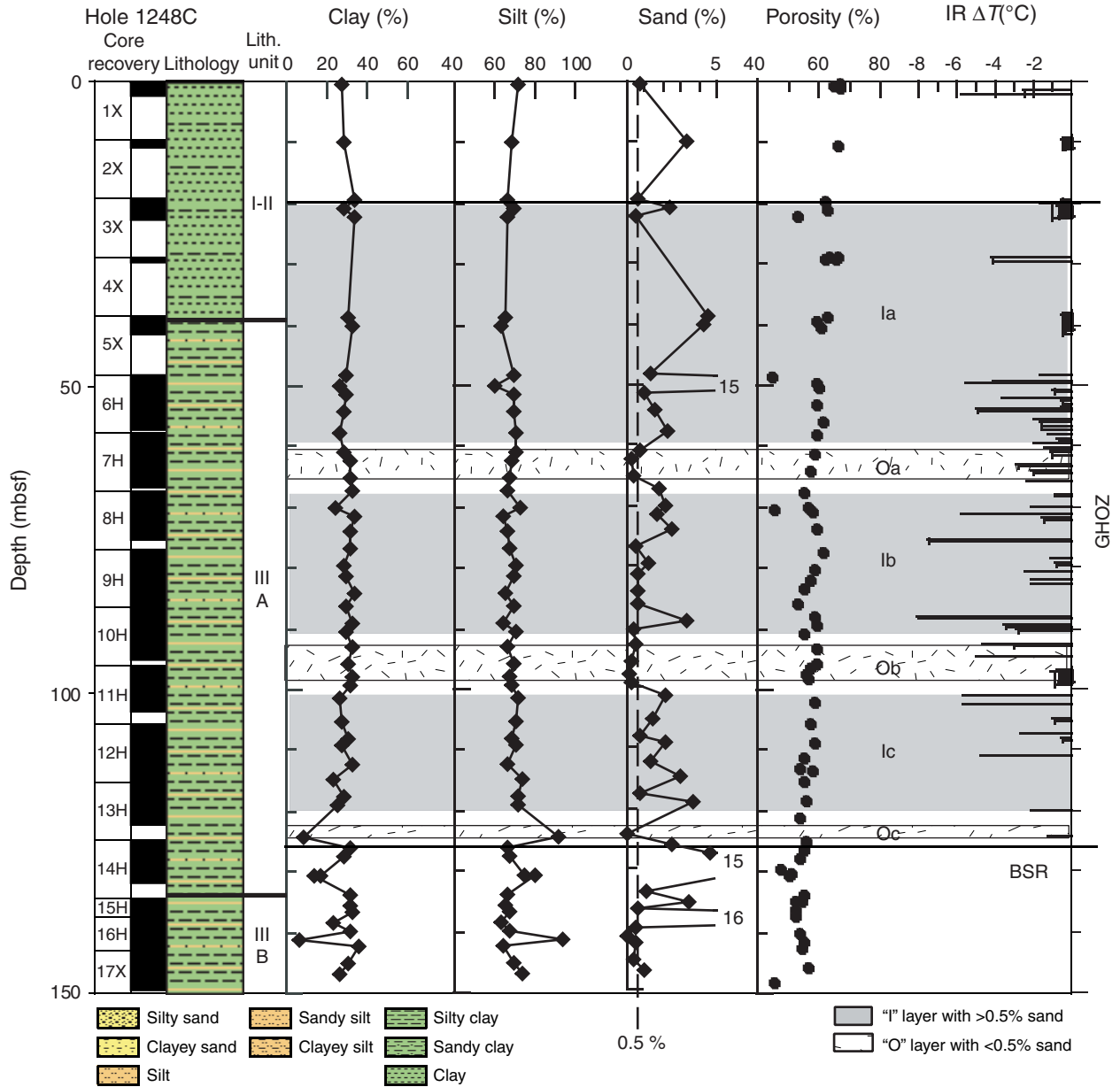


Figure F7. Downhole variation of sediment grain size within the gas hydrate occurrence zone (GHOZ) in Hole 1249C correlated with infrared thermal anomalies (IR) and porosity. BSR = bottom-simulating reflector. IR and porosity data, core recovery, lithologic units, and legends for lithology are from Shipboard Scientific Party (2003).

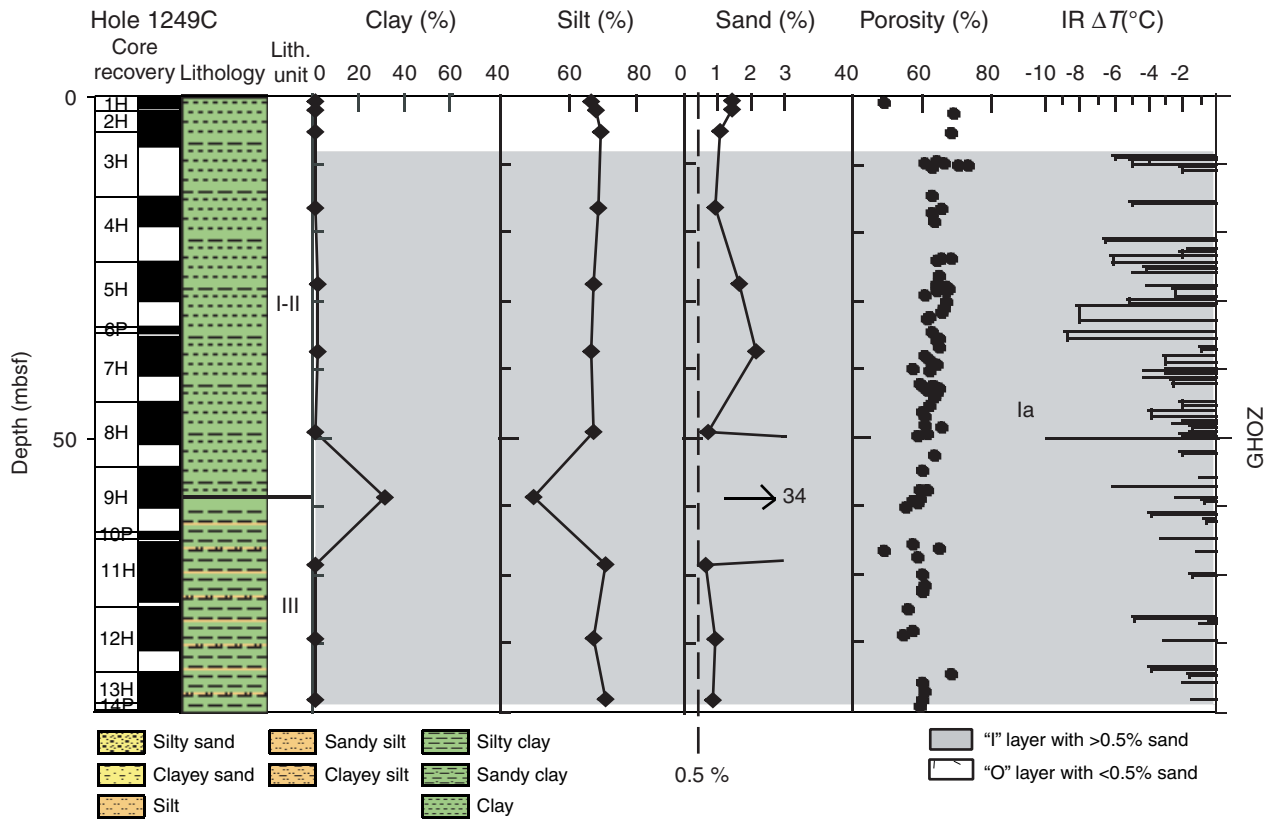


Figure F8. Downhole variation of sediment grain size within the gas hydrate occurrence zone (GHOZ) in Hole 1250C correlated with infrared thermal anomalies (IR) and porosity. BSR = bottom-simulating reflector. IR and porosity data, core recovery, lithologic units, and legends for lithology are from Shipboard Scientific Party (2003).

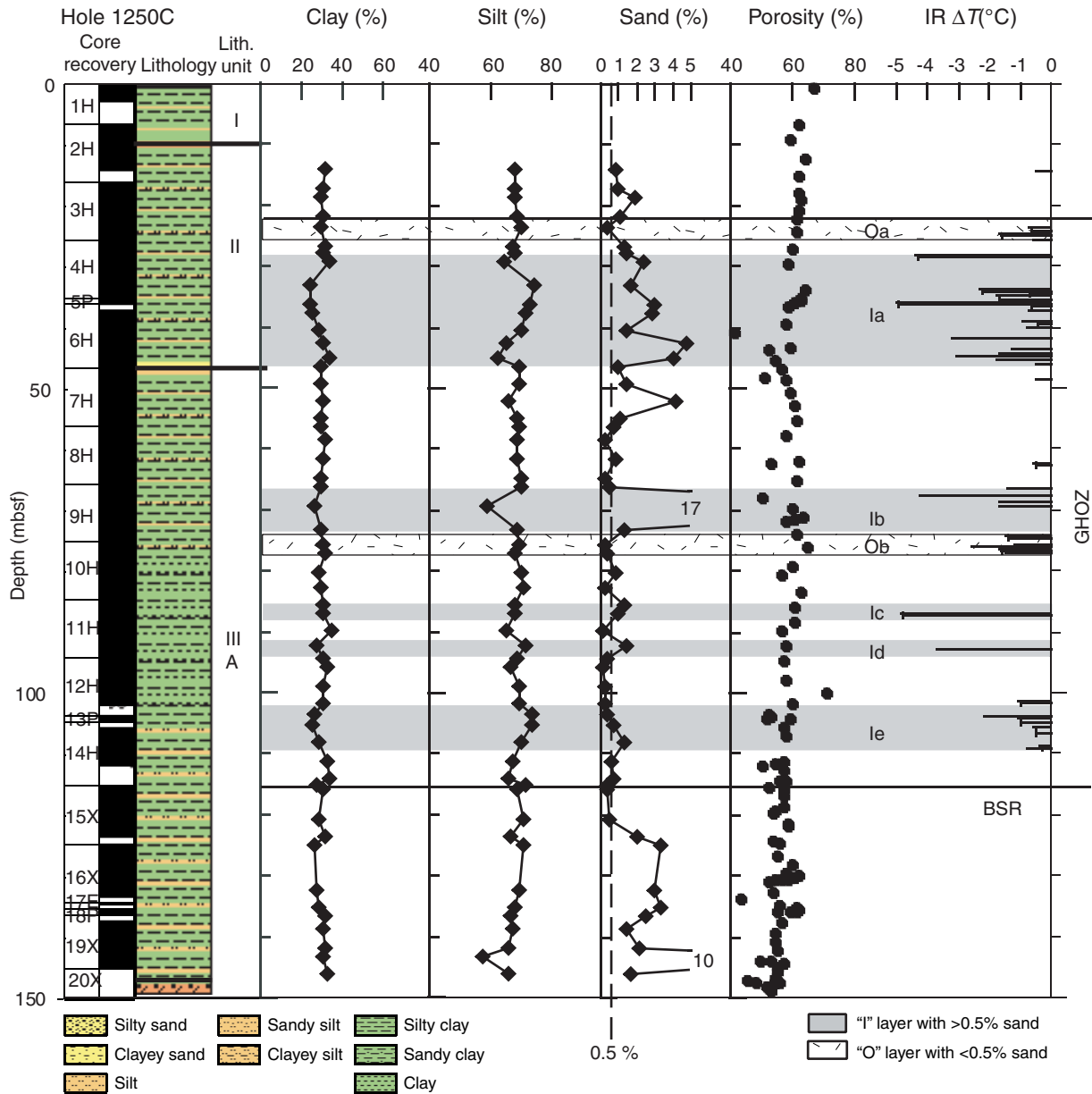


Figure F9. Downhole variation of sediment grain size within the gas hydrate occurrence zone (GHOZ) in Hole 1251B correlated with infrared thermal anomalies (IR) and porosity. BSR = bottom-simulating reflector. IR and porosity data, core recovery, lithologic units, and legends for lithology are from Shipboard Scientific Party (2003).

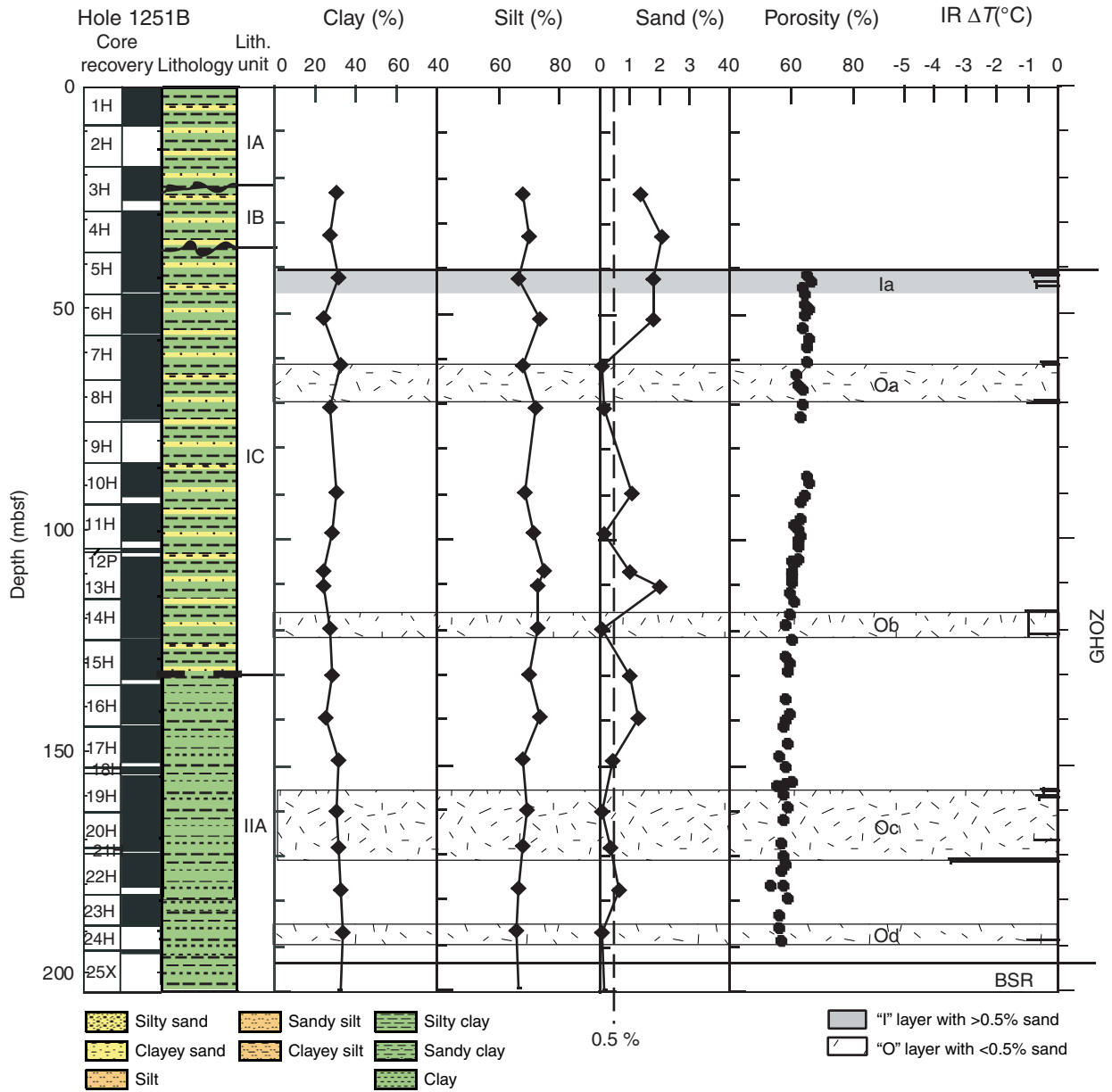


Figure F10. Downhole variation of sediment grain size within the gas hydrate occurrence zone (GHOZ) in Hole 1252C correlated with infrared thermal anomalies (IR) and porosity. BSR = bottom-simulating reflector. IR and porosity data, core recovery, lithologic units, and legends for lithology are from Shipboard Scientific Party (2003).

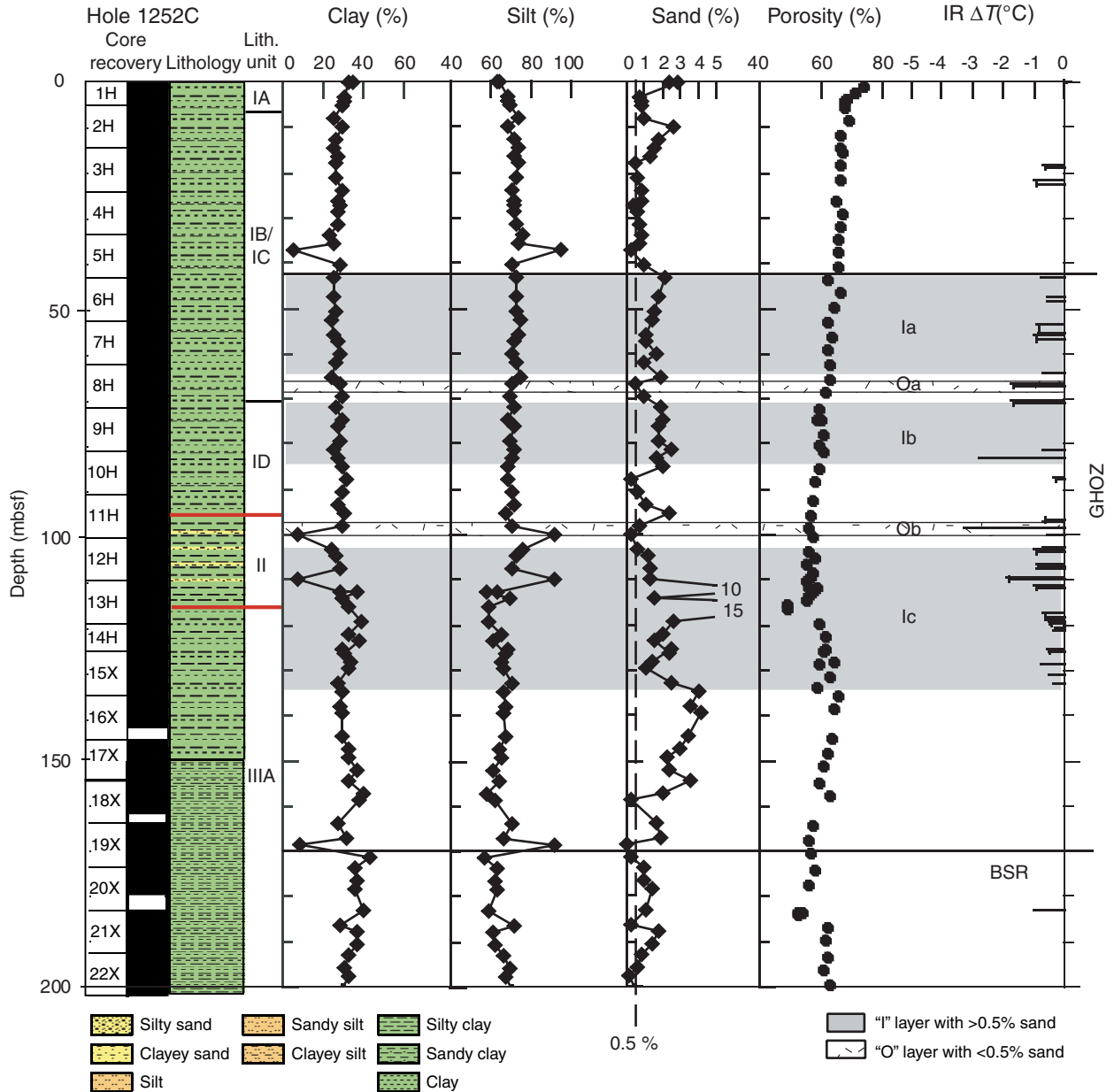


Figure F11. Statistical correlation of grain sizes and gas hydrate occurrence indicated by IR record in Holes 1244C, 1245B, 1246B, 1248B, 1249C, 1250C, 1251B, and 1252A.

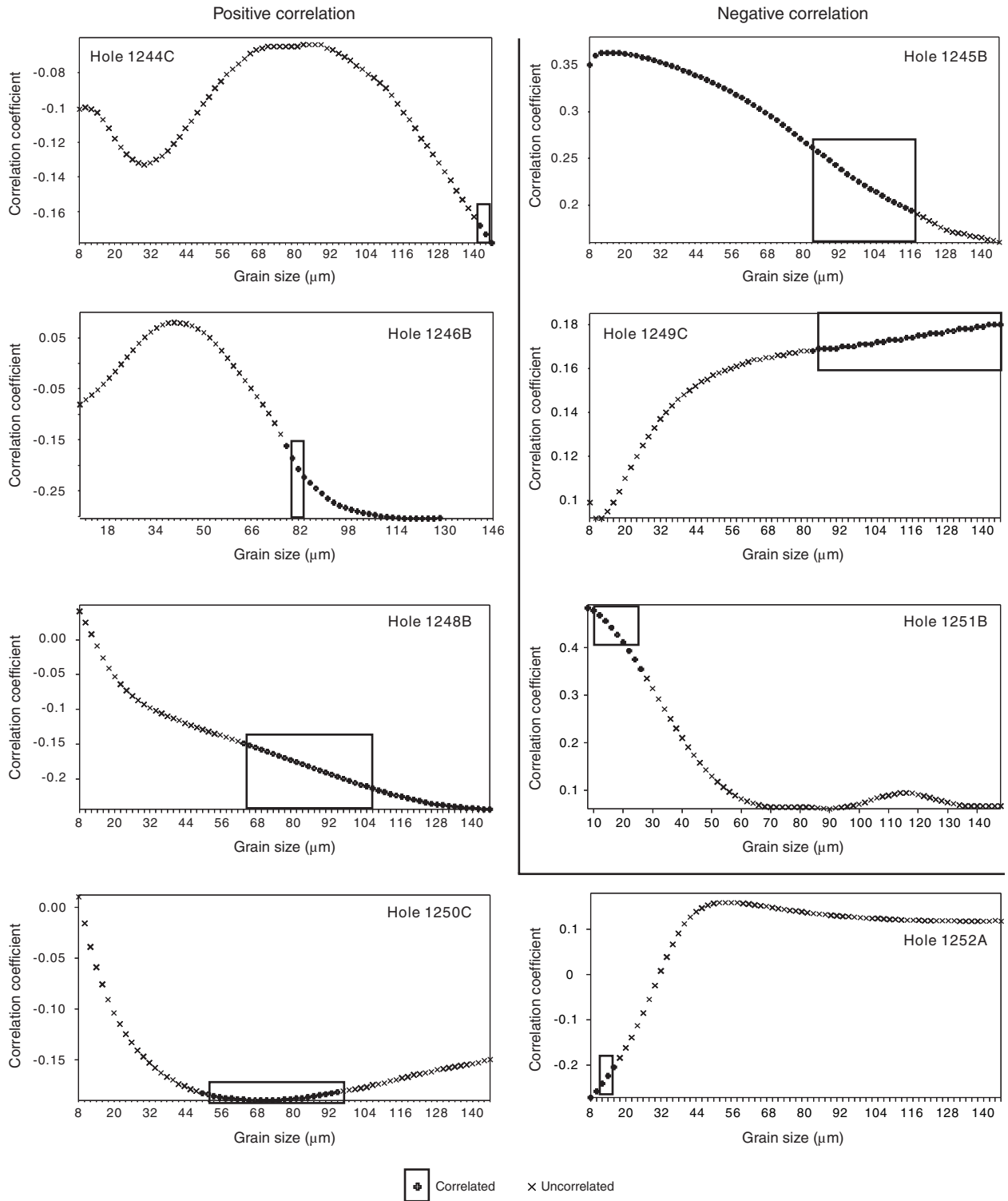


Figure F12. A. Grain-size ranges correlated to gas hydrate occurrence at Leg 204 sites. B. Geographical location of sites on Hydrate Ridge. GHY = gas hydrate.

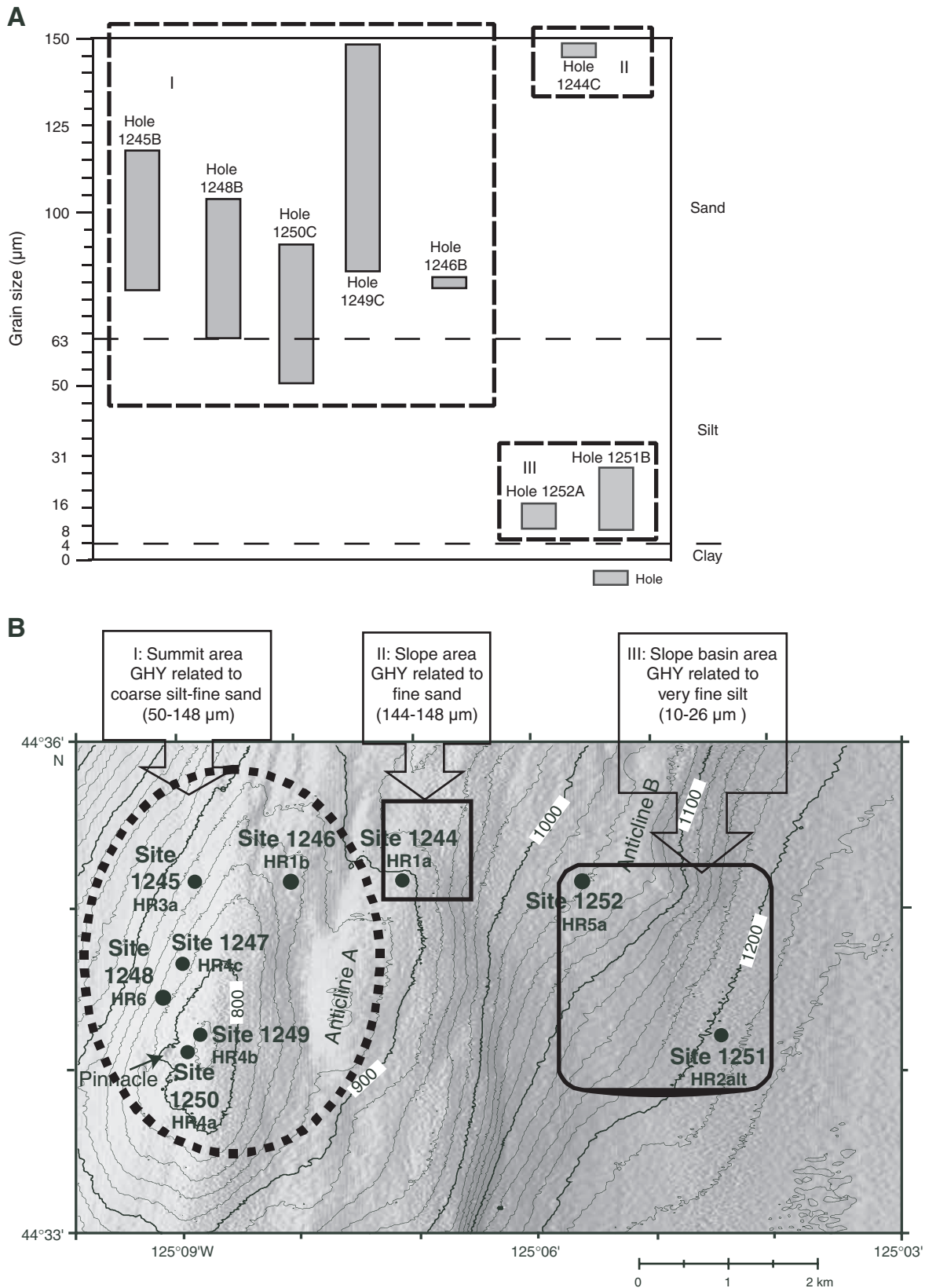


Table T1. Site location and sample data, Leg 204.

Site	Location	Water depth (m)	BSR depth (mbsf)	<i>N</i>
1244	44.586°N, 125.119°W	890	125	16
1245	44.586°N, 125.148°W	870	134	58
1246	44.586°N, 125.135°W	848	114	50
1248	44.574°N, 125.153°W	832	124	45
1249	44.57°N, 125.148°W	778	115	13
1250	44.569°N, 125.149°W	782	114	42
1251	44.57°N, 125.074°W	1216	196	20
1252	44.486°N, 125.094°W	1039	170	75

Notes: From Shipboard Scientific Party, 2003. BSR = bottom-simulating reflector, *N* = number of samples analyzed.

Table T2. Grain-size range classes.

Fraction	Size range (μm)	Subfraction	Size range (μm)
Sand	2000.0~63.0	Fine sand	250.0~125.0
		Very fine sand	125.0~63.0
Silt	63.0~3.9	Coarse silt	63.0~31.0
		Medium silt	31.0~15.6
		Fine silt	15.6~7.8
		Very fine silt	7.8~3.9
Clay	<3.9		

Note: From the classification of Friedman and Sanders (1978).

Table T3. IR anomalies in Leg 204 holes. (See table note. Continued on next page.)

Hole	ΔT (°C)	Top (cm)	Bottom (cm)	Hole	ΔT (°C)	Top (cm)	Bottom (cm)	Hole	ΔT (°C)	Top (cm)	Bottom (cm)	
1244C	-0.5	22.90	23.20	1246B	-4.4	85.95	86.15	1248B	-0.6	115.60	115.70	
	-0.5	44.25	44.65		-3	87.60	87.70		-0.5	116.70	116.80	
	-1.2	47.50	47.70		-1.5	88.20	88.35		-0.5	9.60	10.88	
	-2.7	48.01	48.15		-1.3	89.60	89.80		-0.5	19.20	20.00	
	-2.7	49.15	49.32		-1.4	90.55	90.75		-1.6	20.00	20.10	
	-1.1	49.50	49.59		-1.2	91.35	91.40		-1	20.10	22.68	
	-3.8	49.99	50.16		-4	91.70	91.80		-4.1	28.80	29.65	
	-0.7	55.73	56.10		-0.9	99.80	99.87		-0.5	38.40	41.40	
	-1.5	57.90	58.24		-2.9	101.90	102.15		-1.6	48.10	48.30	
	-6.9	59.30	59.70		-1.5	108.25	108.40		-4	49.30	49.40	
	-2.7	62.10	62.17		-2.6	113.40	113.55		-5.5	49.70	49.77	
	-1.4	0.00	0.40		-0.9	115.38	115.42		-0.9	50.70	51.20	
	-1.7	65.40	65.50		-0.5	116.90	116.95		-3.6	52.10	52.20	
	-2.4	65.56	65.79		-1	117.55	117.65		-0.4	52.30	53.10	
	-2	68.53	68.56		-1.5	119.75	119.85		-0.5	53.50	53.70	
	-1.4	70.03	70.05		-2.1	121.30	121.50		-4.9	54.00	54.20	
	-1.3	70.40	70.45		-6	129.10	129.40		-1.9	55.60	55.70	
	-0.8	61.65	61.74		1249C	-0.5	16.00		17.40	-1.6	56.00	56.80
	-5.4	62.40	62.50			-1.8	18.00		19.00	-1.4	57.30	57.40
	-5.1	73.95	74.25			-1.4	19.70		21.90	-1.1	58.10	58.20
	-1.1	79.90	79.95			-0.3	25.00		29.40	-0.7	58.80	59.20
	-1.3	82.67	82.75			-0.4	31.40		32.60	-1.9	59.40	59.60
	-1.2	83.30	83.65			-0.3	34.50		35.00	-1.3	60.20	60.35
	-0.8	85.65	85.72			-0.7	36.00		36.10	-1	60.40	60.55
	-2.9	86.75	86.90			-1.8	38.10		38.40	-1	61.00	61.50
	-0.7	89.31	89.65			-1	40.00		41.00	-2.8	63.20	63.35
	-1	90.35	90.44			-0.7	42.20		42.30	-2	64.20	64.50
	-2.3	90.69	90.93			-0.6	43.40		43.50	-2.2	65.70	65.90
	-4.9	92.05	92.48			-0.9	44.60		44.80	-0.8	65.95	66.00
	-0.6	92.96	93.01			-0.5	46.20		46.40	-0.8	67.90	68.00
	-0.8	93.68	93.77			-1.2	49.70		49.80	-0.8	68.20	68.40
	-1.1	94.30	94.48			-1.3	51.00		51.50	-2	69.90	70.00
-0.8	95.15	95.23	-0.6	53.10		53.30	-5.7	71.10	71.30			
-0.8	97.69	97.78	-1.5	56.80		57.30	-1.5	72.00	72.10			
-1.1	98.08	98.15	-0.6	59.35		59.45	-7.4	75.20	75.60			
-0.9	98.91	99.32	-1.4	61.50		61.60	-1	78.50	78.65			
-3	100.06	100.16	-0.3	61.80		61.90	-0.8	79.40	79.60			
-1.9	100.30	100.37	-0.7	63.00		63.40	-2.3	80.50	80.60			
-0.7	100.88	100.93	-4	66.00		66.50	-2	81.90	82.00			
-1	101.31	101.67	-1	66.75		67.10	-2	82.80	82.90			
-1.8	113.78	113.90	-1.4	67.20		67.40	-2	82.80	82.90			
-0.7	114.30	114.41	-0.7	71.40		71.80	-8.1	88.10	88.40			
-1.5	114.66	114.74	-0.6	72.10		72.40	-3.5	89.50	89.70			
-1.7	114.98	115.05	-2.1	72.80		73.30	-2.8	90.30	90.50			
-0.5	115.70	115.77	-0.4	74.90		75.00	-4.6	92.50	92.55			
-0.8	116.75	117.00	-0.4	75.90		76.00	-3	92.70	92.80			
-1.5	118.08	118.29	-1.8	76.10		77.00	-4.9	94.75	94.80			
-1.7	118.58	118.29	-0.9	78.20		79.10	-1	97.20	97.25			
-1.7	118.58	118.82	-2	80.10		81.20	-0.9	97.26	99.40			
-1.7	121.25	121.25	-1.2	81.80	81.90	-5.6	101.00	101.10				
1245B	-2.1	51.50	51.60	-0.8	82.10	82.30	-5.6	102.50	102.60			
	-2.5	51.80	51.85	-1.5	84.30	84.50	-0.9	105.00	105.25			
	-1.5	52.40	52.50	-3	85.70	86.00	-2.6	107.40	107.50			
	-2.5	52.80	53.10	-2.5	88.00	88.20	-0.5	108.27	108.32			
	-1	53.95	54.00	-1.5	89.00	89.20	-4.7	110.90	111.00			
	-9.4	54.35	54.50	-1	86.10	86.20	-2	120.05	120.20			
	-4.1	57.10	57.30	-1.1	90.30	90.70	-1.1	124.15	124.25			
	-6	62.10	62.60	-1	92.70	92.90	1249C	-6	9.00	9.10		
	-0.7	64.50	64.80	-0.6	93.90	94.00		-4	9.11	9.55		
	-3.4	70.85	71.20	-4.4	96.80	97.10		-5	9.65	10.25		
	-0.8	73.90	73.95	-1.6	99.70	100.00		-2	10.40	10.95		
	-0.8	75.20	75.27	-6.6	104.80	105.30		-5	15.50	15.80		
	-1.6	78.30	78.55	-1.8	106.10	106.50		-6.5	20.90	21.09		
	-1.5	79.20	79.25	-0.6	107.70	107.80		-1.7	22.60	22.80		
	-1	79.65	79.80	-3.1	109.20	109.70		-2.1	22.90	23.55		
	-1.5	81.00	81.10	-0.8	109.80	110.40		-6.1	23.57	24.48		
	-2.4	82.90	83.25	-0.8	111.00	111.20		-4.1	25.10	25.45		
	-4.8	84.70	84.75	-0.7	114.20	114.30		-4.9	26.05	26.23		
	-2.6	94.40	94.50	-0.8	115.00	115.10						

Table T3 (continued).

Hole	ΔT (°C)	Top (cm)	Bottom (cm)	Hole	ΔT (°C)	Top (cm)	Bottom (cm)	Hole	ΔT (°C)	Top (cm)	Bottom (cm)
	-4	28.00	28.20		-2.2	33.90	34.10		-0.6	157.00	157.10
	-2.5	28.40	29.60		-0.7	34.30	34.50		-0.7	166.70	166.80
	-5.1	30.05	30.75		-1.7	34.75	35.65		-3.5	171.00	171.20
	-8	30.60	33.10		-4.9	35.85	36.10		-0.9	188.50	188.60
	-8.8	34.70	35.40		-0.6	36.30	36.70		-0.7	213.80	214.10
	-1	36.90	37.15		-0.6	37.35	37.42		-0.9	350.10	350.10
	-3	38.05	38.85		-0.8	38.97	39.00	1252A	-0.6	18.50	19.00
	-2.9	39.90	39.96		-0.4	39.25	39.28		-0.9	21.40	22.50
	-4.2	40.30	40.40		-0.7	40.18	40.23		-0.7	43.00	43.09
	-2.9	40.60	40.70		-3.1	41.86	41.90		-0.5	47.40	47.61
	-4.1	41.15	41.25		-1.2	43.62	43.80		-0.5	48.42	48.50
	-2.6	41.40	42.00		-1.6	44.25	44.37		-0.8	53.70	55.35
	-2	44.80	45.30		-3	44.70	44.76		-0.9	55.70	56.80
	-3.8	45.80	46.85		-1.7	45.40	45.46		-0.6	64.20	64.50
	-1.9	47.40	47.65		-0.4	46.22	46.30		-1.7	66.50	67.32
	-2.5	47.70	47.75		-0.4	48.60	48.65		-1.7	70.64	70.71
	-1.5	48.20	48.60		-0.5	62.40	62.50		-0.6	81.00	81.11
	-1.5	49.00	49.10		-1.3	66.39	66.57		-2.7	83.06	83.25
	-2	49.50	49.60		-4.2	67.45	67.64		-0.3	87.47	87.56
	-1	49.40	49.70		-1.6	68.60	68.67		-0.6	97.10	96.83
	-2.1	52.10	52.30		-1.6	69.41	69.44		-3.2	98.45	98.50
	-0.9	55.70	55.85		-1.4	74.30	74.65		-0.5	100.08	100.12
	-6	56.95	57.10		-1.1	75.55	75.63		-0.6	102.90	102.94
	-2.4	58.50	58.57		-1	75.78	75.80		-0.9	103.43	103.64
	-0.8	59.05	59.15		-2.5	75.92	76.06		-0.4	103.89	103.90
	-3.8	60.98	61.10		-1.6	76.47	76.60		-0.8	106.80	106.86
	-0.7	61.65	62.00		-1.4	77.05	77.16		-0.8	107.39	107.42
	-3.2	64.75	64.80		-4.8	87.10	87.20		-1.8	109.48	109.65
	-1.1	66.60	66.66		-1.5	92.90	92.95		-0.9	111.50	111.85
	-3	67.00	67.10		-3.6	93.05	93.10		-0.6	117.50	118.40
	-1.5	69.65	69.90		-1	101.50	101.59		-0.5	118.90	119.10
	-4.8	76.05	76.25		-2.1	103.70	103.90		-0.4	119.40	119.75
	-0.4	76.60	76.70		-1	104.25	104.90		-0.2	120.60	120.67
	-0.9	77.05	77.15		-0.5	105.70	106.70		-0.3	121.20	121.25
	-3.8	83.25	83.60		-0.3	108.80	109.00		-0.5	125.25	125.70
	-1.6	84.15	84.55		-0.7	109.20	109.30		-0.7	128.55	128.62
	-1.9	85.55	88.06						-0.4	131.05	131.14
	-1.3	88.00	88.06	1251B	-0.8	41.30	42.00		-0.3	132.88	132.94
1250C	-0.5	14.27	14.50		-0.7	43.00	44.00		-0.9	183.15	183.22
	-0.6	23.68	24.19		-0.5	61.20	61.30				
	-1.6	24.65	24.85		-0.7	69.60	69.70				
	-0.5	25.60	25.65		-0.9	69.90	70.00				
	-4.3	28.28	28.65		-1	116.00	121.00				
					-0.5	155.60	155.70				

Note: From Shipboard Scientific Party (2003).

Table T4. Results of the bivariate correlations procedure. (See table notes. Continued on next four pages.)

Grain size interval (µm)	Temperature	Hole								
		1244C	1245B	1246B	1248B	1249C	1250C	1251B	1252A	
		Pearson correlation	1.000	1.000	1.000	1.000	1.000	1.000	1.000	1.000
		Significance (1-tailed)	—	—	—	—	—	—	—	—
		N	97	75	124	124	97	83	23	73
8–10	LINT(VAR00001)	Pearson correlation	-0.101	0.35†	-0.081	0.041	0.099	0.01	0.483	-0.272
		Significance (1-tailed)	0.163	0.001	0.186	0.327	0.168	0.464	0.01	0.01
		N	97	75	124	124	97	83	23	73
10–12	LINT(VAR00002)	Pearson correlation	-0.100	0.36†	-0.071	0.025	0.092	-0.016	0.478*	-0.258*
		Significance (1-tailed)	0.164	0.001	0.216	0.392	0.185	0.441	0.011	0.014
		N	97	75	124	124	97	83	23	73
12–14	LINT(VAR00003)	Pearson correlation	-0.101	0.363†	-0.062	0.008	0.092	-0.039	0.468*	-0.241*
		Significance (1-tailed)	0.163	0.001	0.248	0.466	0.186	0.362	0.012	0.02
		N	97	75	124	124	97	83	23	73
14–16	LINT(VAR00004)	Pearson correlation	-0.103	0.363†	-0.052	-0.009	0.095	-0.059	0.456*	-0.224*
		Significance (1-tailed)	0.158	0.001	0.283	0.459	0.178	0.297	0.014	0.029
		N	97	75	124	124	97	83	23	73
16–18	LINT(VAR00005)	Pearson correlation	-0.107	0.363†	-0.041	-0.026	0.099	-0.076	0.442*	-0.205*
		Significance (1-tailed)	0.149	0.001	0.324	0.388	0.167	0.246	0.017	0.041
		N	97	75	124	124	97	83	23	73
18–20	LINT(VAR00006)	Pearson correlation	-0.112	0.363†	-0.029	-0.041	0.104	-0.091	0.427*	-0.184
		Significance (1-tailed)	0.137	0.001	0.373	0.327	0.154	0.206	0.021	0.059
		N	97	75	124	124	97	83	23	73
20–22	LINT(VAR00007)	Pearson correlation	-0.118	0.362†	-0.016	-0.053	0.11	-0.104	0.411*	-0.162
		Significance (1-tailed)	0.126	0.001	0.429	0.278	0.142	0.175	0.026	0.085
		N	97	75	124	124	97	83	23	73
22–24	LINT(VAR00008)	Pearson correlation	-0.123	0.361†	-0.002	-0.064	0.115	-0.115	0.393*	-0.139
		Significance (1-tailed)	0.115	0.001	0.49	0.239	0.131	0.15	0.032	0.121
		N	97	75	124	124	97	83	23	73
24–26	LINT(VAR00009)	Pearson correlation	-0.127	0.36†	0.012	-0.073	0.12	-0.125	0.375*	-0.113
		Significance (1-tailed)	0.107	0.001	0.448	0.209	0.12	0.13	0.039	0.17
		N	97	75	124	124	97	83	23	73
26–28	LINT(VAR00010)	Pearson correlation	-0.130	0.358†	0.026	-0.081	0.125	-0.133	0.355*	-0.085
		Significance (1-tailed)	0.102	0.001	0.388	0.186	0.111	0.115	0.048	0.237
		N	97	75	124	124	97	83	23	73
28–30	LINT(VAR00011)	Pearson correlation	-0.132	0.357†	0.039	-0.087	0.129	-0.141	0.335	-0.055
		Significance (1-tailed)	0.099	0.001	0.334	0.167	0.103	0.102	0.059	0.321
		N	97	75	124	124	97	83	23	73
30–32	LINT(VAR00012)	Pearson correlation	-0.133	0.355†	0.051	-0.093	0.133	-0.147	0.314	-0.024
		Significance (1-tailed)	0.098	0.001	0.288	0.153	0.097	0.092	0.072	0.42
		N	97	75	124	124	97	83	23	73
32–34	LINT(VAR00013)	Pearson correlation	-0.132	0.353†	0.061	-0.098	0.137	-0.153	0.292	0.008
		Significance (1-tailed)	0.099	0.001	0.251	0.14	0.091	0.083	0.088	0.473
		N	97	75	124	124	97	83	23	73
34–36	LINT(VAR00014)	Pearson correlation	-0.130	0.351†	0.069	-0.102	0.14	-0.158	0.271	0.039
		Significance (1-tailed)	0.102	0.001	0.223	0.13	0.086	0.076	0.105	0.373
		N	97	75	124	124	97	83	23	73
36–38	LINT(VAR00015)	Pearson correlation	-0.128	0.349†	0.075	-0.106	0.143	-0.163	0.25	0.067
		Significance (1-tailed)	0.106	0.001	0.204	0.121	0.081	0.071	0.125	0.287
		N	97	75	124	124	97	83	23	73

Table T4 (continued).

Grain size interval (µm)	Temperature		Hole							
			1244C	1245B	1246B	1248B	1249C	1250C	1251B	1252A
38–40	LINT(VAR00016)	Pearson correlation	-0.125	0.347 [†]	0.079	-0.110	0.146	-0.167	0.23	0.091
		Significance (1-tailed)	0.112	0.001	0.193	0.113	0.077	0.066	0.146	0.221
		N	97	75	124	124	97	83	23	73
40–42	LINT(VAR00017)	Pearson correlation	-0.121	0.344 [†]	0.08	-0.113	0.148	-0.170	0.21	0.112
		Significance (1-tailed)	0.119	0.001	0.189	0.106	0.074	0.062	0.168	0.174
		N	97	75	124	124	97	83	23	73
42–44	LINT(VAR00018)	Pearson correlation	-0.117	0.342 [†]	0.079	-0.116	0.15	-0.174	0.191	0.127
		Significance (1-tailed)	0.127	0.001	0.191	0.099	0.071	0.058	0.191	0.142
		N	97	75	124	124	97	83	23	73
44–46	LINT(VAR00019)	Pearson correlation	-0.112	0.339 [†]	0.077	-0.120	0.152	-0.176	0.174	0.139
		Significance (1-tailed)	0.137	0.001	0.199	0.093	0.069	0.055	0.213	0.12
		N	97	75	124	124	97	83	23	73
46–48	LINT(VAR00020)	Pearson correlation	-0.108	0.337 [†]	0.073	-0.123	0.154	-0.179	0.158	0.147
		Significance (1-tailed)	0.147	0.002	0.212	0.087	0.066	0.053	0.236	0.107
		N	97	75	124	124	97	83	23	73
48–50	LINT(VAR00021)	Pearson correlation	-0.103	0.334 [†]	0.067	-0.126	0.155	-0.181	0.143	0.153
		Significance (1-tailed)	0.158	0.002	0.23	0.082	0.064	0.051	0.257	0.098
		N	97	75	124	124	97	83	23	73
50–52	LINT(VAR00022)	Pearson correlation	-0.098	0.331 [†]	0.06	-0.129	0.157	-0.183*	0.13	0.157
		Significance (1-tailed)	0.17	0.002	0.255	0.077	0.063	0.049	0.278	0.093
		N	97	75	124	124	97	83	23	73
52–54	LINT(VAR00023)	Pearson correlation	-0.094	0.328 [†]	0.05	-0.132	0.158	-0.184*	0.118	0.159
		Significance (1-tailed)	0.181	0.002	0.29	0.072	0.061	0.048	0.296	0.09
		N	97	75	124	124	97	83	23	73
54–56	LINT(VAR00024)	Pearson correlation	-0.089	0.325 [†]	0.038	-0.135	0.159	-0.186*	0.107	0.159
		Significance (1-tailed)	0.193	0.002	0.336	0.068	0.06	0.046	0.314	0.089
		N	97	75	124	124	97	83	23	73
56–58	LINT(VAR00025)	Pearson correlation	-0.085	0.322 [†]	0.025	-0.137	0.16	-0.187*	0.097	0.159
		Significance (1-tailed)	0.204	0.002	0.392	0.064	0.058	0.045	0.33	0.089
		N	97	75	124	124	97	83	23	73
58–60	LINT(VAR00026)	Pearson correlation	-0.081	0.318 [†]	0.01	-0.140	0.161	-0.188*	0.089	0.159
		Significance (1-tailed)	0.214	0.003	0.454	0.06	0.057	0.045	0.343	0.09
		N	97	75	124	124	97	83	23	73
60–62	LINT(VAR00027)	Pearson correlation	-0.078	0.315 [†]	-0.005	-0.143	0.162	-0.188*	0.082	0.157
		Significance (1-tailed)	0.225	0.003	0.48	0.056	0.056	0.044	0.355	0.092
		N	97	75	124	124	97	83	23	73
62–64	LINT(VAR00028)	Pearson correlation	-0.075	0.311 [†]	-0.019	-0.146	0.163	-0.189*	0.077	0.156
		Significance (1-tailed)	0.234	0.003	0.417	0.053	0.055	0.044	0.363	0.094
		N	97	75	124	124	97	83	23	73
64–66	LINT(VAR00029)	Pearson correlation	-0.072	0.307 [†]	-0.034	-0.149*	0.164	-0.189*	0.073	0.154
		Significance (1-tailed)	0.242	0.004	0.356	0.049	0.055	0.043	0.37	0.096
		N	97	75	124	124	97	83	23	73
66–68	LINT(VAR00030)	Pearson correlation	-0.069	0.303 [†]	-0.049	-0.152*	0.164	-0.190*	0.069	0.152
		Significance (1-tailed)	0.25	0.004	0.295	0.046	0.054	0.043	0.377	0.099
		N	97	75	124	124	97	83	23	73
68–70	LINT(VAR00031)	Pearson correlation	-0.067	0.299 [†]	-0.065	-0.155*	0.165	-0.190*	0.066	0.151
		Significance (1-tailed)	0.256	0.005	0.236	0.043	0.053	0.043	0.382	0.102
		N	97	75	124	124	97	83	23	73

Table T4 (continued).

Grain size interval (µm)	Temperature		Hole							
			1244C	1245B	1246B	1248B	1249C	1250C	1251B	1252A
70–72	LINT(VAR00032)	Pearson correlation	-0.066	0.295 [†]	-0.081	-0.158*	0.165	-0.190*	0.065	0.148
		Significance (1-tailed)	0.26	0.005	0.185	0.04	0.053	0.043	0.385	0.105
		N	97	75	124	124	97	83	23	73
72–74	LINT(VAR00033)	Pearson correlation	-0.065	0.291 [†]	-0.098	-0.161*	0.166	-0.190*	0.065	0.146
		Significance (1-tailed)	0.263	0.006	0.14	0.037	0.052	0.043	0.385	0.108
		N	97	75	124	124	97	83	23	73
74–76	LINT(VAR00034)	Pearson correlation	-0.065	0.286 [†]	-0.117	-0.164*	0.166	-0.190*	0.065	0.144
		Significance (1-tailed)	0.265	0.006	0.098	0.034	0.052	0.043	0.384	0.111
		N	97	75	124	124	97	83	23	73
76–78	LINT(VAR00035)	Pearson correlation	-0.065	0.281 [†]	-0.139	-0.167*	0.167	-0.190*	0.065	0.142
		Significance (1-tailed)	0.265	0.007	0.062	0.032	0.051	0.043	0.384	0.115
		N	97	75	124	124	97	83	23	73
78–80	LINT(VAR00036)	Pearson correlation	-0.065	0.276 [†]	-0.162*	-0.170*	0.167	-0.189*	0.065	0.141
		Significance (1-tailed)	0.264	0.008	0.036	0.03	0.051	0.043	0.384	0.118
		N	97	75	124	124	97	83	23	73
80–82	LINT(VAR00037)	Pearson correlation	-0.065	0.271 [†]	-0.186*	-0.173*	0.168	-0.189*	0.064	0.139
		Significance (1-tailed)	0.264	0.009	0.019	0.028	0.05	0.044	0.385	0.121
		N	97	75	124	124	97	83	23	73
82–84	LINT(VAR00038)	Pearson correlation	-0.065	0.266*	-0.207*	-0.176*	0.168	-0.188*	0.063	0.137
		Significance (1-tailed)	0.265	0.011	0.011	0.026	0.05	0.044	0.387	0.124
		N	97	75	124	124	97	83	23	73
84–86	LINT(VAR00039)	Pearson correlation	-0.064	0.262*	-0.223 [†]	-0.179*	0.168*	-0.188*	0.062	0.135
		Significance (1-tailed)	0.266	0.012	0.006	0.024	0.05	0.045	0.389	0.127
		N	97	75	124	124	97	83	23	73
86–88	LINT(VAR00040)	Pearson correlation	-0.064	0.257*	-0.234 [†]	-0.182*	0.169*	-0.187*	0.061	0.134
		Significance (1-tailed)	0.267	0.013	0.004	0.022	0.049	0.046	0.39	0.129
		N	97	75	124	124	97	83	23	73
88–90	LINT(VAR00041)	Pearson correlation	-0.064	0.253*	-0.245 [†]	-0.185*	0.169*	-0.186*	0.063	0.133
		Significance (1-tailed)	0.267	0.014	0.003	0.02	0.049	0.046	0.388	0.132
		N	97	75	124	124	97	83	23	73
90–92	LINT(VAR00042)	Pearson correlation	-0.064	0.248*	-0.255 [†]	-0.188*	0.169*	-0.185*	0.064	0.131
		Significance (1-tailed)	0.265	0.016	0.002	0.018	0.049	0.047	0.386	0.134
		N	97	75	124	124	97	83	23	73
92–94	LINT(VAR00043)	Pearson correlation	-0.066	0.243*	-0.265 [†]	-0.191*	0.169*	-0.184*	0.066	0.13
		Significance (1-tailed)	0.262	0.018	0.001	0.017	0.049	0.048	0.383	0.136
		N	97	75	124	124	97	83	23	73
94–96	LINT(VAR00044)	Pearson correlation	-0.067	0.238*	-0.273 [†]	-0.194*	0.17*	-0.183*	0.068	0.129
		Significance (1-tailed)	0.256	0.02	0.001	0.015	0.048	0.049	0.379	0.138
		N	97	75	124	124	97	83	23	73
96–98	LINT(VAR00045)	Pearson correlation	-0.069	0.233*	-0.279 [†]	-0.197*	0.17*	-0.182*	0.071	0.128
		Significance (1-tailed)	0.251	0.022	0.001	0.014	0.048	0.05	0.374	0.14
		N	97	75	124	124	97	83	23	73
98–100	LINT(VAR00046)	Pearson correlation	-0.071	0.229*	-0.283 [†]	-0.200*	0.17*	-0.181	0.075	0.127
		Significance (1-tailed)	0.244	0.024	0.001	0.013	0.048	0.051	0.366	0.142
		N	97	75	124	124	97	83	23	73
100–102	LINT(VAR00047)	Pearson correlation	-0.073	0.225*	-0.287 [†]	-0.203*	0.171*	-0.180	0.08	0.126
		Significance (1-tailed)	0.237	0.026	0.001	0.012	0.047	0.052	0.358	0.144
		N	97	75	124	124	97	83	23	73

Table T4 (continued).

Grain size interval (µm)	Temperature		Hole							
			1244C	1245B	1246B	1248B	1249C	1250C	1251B	1252A
102–104	LINT(VAR00048)	Pearson correlation	-0.076	0.221*	-0.290†	-0.206*	0.171*	-0.179	0.084	0.125
		Significance (1-tailed)	0.23	0.028	0.001	0.011	0.047	0.053	0.352	0.146
		N	97	75	124	124	97	83	23	73
104–106	LINT(VAR00049)	Pearson correlation	-0.078	0.217*	-0.293†	-0.209*	0.171*	-0.178	0.087	0.124
		Significance (1-tailed)	0.225	0.03	0	0.01	0.047	0.054	0.346	0.147
		N	97	75	124	124	97	83	23	73
106–108	LINT(VAR00050)	Pearson correlation	-0.081	0.214*	-0.295†	-0.211†	0.172*	-0.177	0.089	0.124
		Significance (1-tailed)	0.216	0.033	0	0.009	0.046	0.055	0.343	0.149
		N	97	75	124	124	97	83	23	73
108–110	LINT(VAR00051)	Pearson correlation	-0.083	0.21*	-0.297†	-0.214†	0.172*	-0.175	0.092	0.123
		Significance (1-tailed)	0.21	0.035	0	0.008	0.046	0.056	0.338	0.15
		N	97	75	124	124	97	83	23	73
110–112	LINT(VAR00052)	Pearson correlation	-0.086	0.206*	-0.300†	-0.217†	0.173*	-0.174	0.095	0.122
		Significance (1-tailed)	0.201	0.038	0	0.008	0.045	0.058	0.334	0.152
		N	97	75	124	124	97	83	23	73
112–114	LINT(VAR00053)	Pearson correlation	-0.089	0.203*	-0.301†	-0.219†	0.173*	-0.173	0.095	0.122
		Significance (1-tailed)	0.192	0.04	0	0.007	0.045	0.059	0.333	0.153
		N	97	75	124	124	97	83	23	73
114–116	LINT(VAR00054)	Pearson correlation	-0.093	0.2*	-0.302†	-0.222†	0.173*	-0.171	0.094	0.121
		Significance (1-tailed)	0.182	0.043	0	0.007	0.045	0.061	0.335	0.154
		N	97	75	124	124	97	83	23	73
116–118	LINT(VAR00055)	Pearson correlation	-0.098	0.197*	-0.303†	-0.224†	0.174*	-0.170	0.091	0.12
		Significance (1-tailed)	0.17	0.045	0	0.006	0.044	0.062	0.34	0.155
		N	97	75	124	124	97	83	23	73
118–120	LINT(VAR00056)	Pearson correlation	-0.103	0.194*	-0.304†	-0.226†	0.174*	-0.168	0.088	0.12
		Significance (1-tailed)	0.159	0.048	0	0.006	0.044	0.064	0.345	0.156
		N	97	75	124	124	97	83	23	73
120–122	LINT(VAR00057)	Pearson correlation	-0.107	0.19	-0.304†	-0.228†	0.175*	-0.167	0.085	0.12
		Significance (1-tailed)	0.148	0.051	0	0.005	0.043	0.066	0.35	0.157
		N	97	75	124	124	97	83	23	73
122–124	LINT(VAR00058)	Pearson correlation	-0.112	0.187	-0.304†	-0.230†	0.175*	-0.165	0.081	0.119
		Significance (1-tailed)	0.137	0.054	0	0.005	0.043	0.067	0.356	0.157
		N	97	75	124	124	97	83	23	73
124–126	LINT(VAR00059)	Pearson correlation	-0.118	0.183	-0.304†	-0.232†	0.176*	-0.164	0.078	0.119
		Significance (1-tailed)	0.126	0.058	0	0.005	0.043	0.069	0.362	0.158
		N	97	75	124	124	97	83	23	73
126–128	LINT(VAR00060)	Pearson correlation	-0.122	0.18	-0.304†	-0.234†	0.176*	-0.163	0.075	0.119
		Significance (1-tailed)	0.117	0.061	0	0.004	0.042	0.071	0.367	0.158
		N	97	75	124	124	97	83	23	73
128–130	LINT(VAR00061)	Pearson correlation	-0.127	0.176	-0.304†	-0.236†	0.176*	-0.162	0.072	0.119
		Significance (1-tailed)	0.107	0.065	0.0003	0.004	0.042	0.072	0.373	0.158
		N	97	75	124	124	97	83	23	73
130–132	LINT(VAR00062)	Pearson correlation	-0.132	0.173	-0.303†	-0.237†	0.177*	-0.160	0.069	0.119
		Significance (1-tailed)	0.099	0.069	0	0.004	0.042	0.074	0.378	0.159
		N	97	75	124	124	97	83	23	73
132–134	LINT(VAR00063)	Pearson correlation	-0.137	0.171	—‡	-0.238†	0.177*	-0.159	0.067	0.119
		Significance (1-tailed)	0.091	0.071	—	0.004	0.041	0.075	0.381	0.159
		N	97	75	124	124	97	83	23	73

Table T4 (continued).

Grain size interval (μm)	Temperature		Hole							
			1244C	1245B	1246B	1248B	1249C	1250C	1251B	1252A
134–136	LINT(VAR00064)	Pearson correlation	-0.142	0.17	—	-0.239 [†]	0.178*	-0.158	0.067	0.118
		Significance (1-tailed)	0.082	0.073	—	0.004	0.041	0.077	0.381	0.159
		N	97	75	124	124	97	83	23	73
136–138	LINT(VAR00065)	Pearson correlation	-0.148	0.169	—	-0.240 [†]	0.178*	-0.157	0.067	0.118
		Significance (1-tailed)	0.075	0.074	—	0.004	0.041	0.078	0.381	0.159
		N	97	75	124	124	97	83	23	73
138–140	LINT(VAR00066)	Pearson correlation	-0.153	0.167	—	-0.241 [†]	0.178*	-0.156	0.067	0.118
		Significance (1-tailed)	0.067	0.076	—	0.004	0.04	0.08	0.381	0.159
		N	97	75	124	124	97	83	23	73
140–142	LINT(VAR00067)	Pearson correlation	-0.158	0.166	—	-0.242 [†]	0.179*	-0.155	0.067	0.118
		Significance (1-tailed)	0.061	0.077	—	0.003	0.04	0.081	0.381	0.16
		N	97	75	124	124	97	83	23	73
142–144	LINT(VAR00068)	Pearson correlation	-0.163	0.165	—	-0.242 [†]	0.179*	-0.154	0.067	0.118
		Significance (1-tailed)	0.055	0.079	—	0.003	0.04	0.083	0.381	0.16
		N	97	75	124	124	97	83	23	73
144–146	LINT(VAR00069)	Pearson correlation	-0.168*	0.163	—	-0.243 [†]	0.18*	-0.153	0.067	0.118
		Significance (1-tailed)	0.05	0.081	—	0.003	0.039	0.084	0.381	0.16
		N	97	75	124	124	97	83	23	73
146–148	LINT(VAR00070)	Pearson correlation	-0.173*	0.162	—	-0.244 [†]	0.18*	-0.151	0.067	0.118
		Significance (1-tailed)	0.045	0.083	—	0.003	0.039	0.086	0.381	0.16
		N	97	75	124	124	97	83	23	73
148–150	LINT(VAR00071)	Pearson correlation	-0.178*	0.16	—	-0.244 [†]	0.18*	-0.150	0.067	0.118
		Significance (1-tailed)	0.04	0.085	—	0.003	0.039	0.087	0.381	0.16
		N	97	75	124	124	97	83	23	73

Notes: * = correlation is significant at the 0.05 level (1-tailed), † = correlation is significant at the 0.01 level (1-tailed). N = number of cases that was used in the correlation. ‡ = no grains >132 μm were found in Hole 1248B, — = no data.

Table T5. Sediment grain-size intervals statistically related to gas hydrate occurrence, Leg 204.

Hole	Range of grain size (μm)
1244C	144–148
1245B	82–120
1246B	78–84
1248C	64–104
1249C	84–148
1250C	50–96
1251B	10–26
1252A	10–16